Geological Society, London, Special Publications

Initial Cenozoic Magmatic Activity in East Africa: New Geochemical Constraints on Magma Distribution within the Eocene Continental Flood Basalt Province

R. Alex Steiner, Tyrone O. Rooney, Guillaume Girard, Nick Rogers, Cynthia Ebinger, Liam Peterson & Rayn Phillips

Full Title: Initial Cenozoic Magmatic Activity in East Africa: New Geochemical Constraints on Magma Distribution within the Eocene Continental Flood Basalt Province

Abbreviated Title: Initial Flood Basalt Magmatism in E. Africa

Authors:

R. Alex Steiner*: Michigan State University; 288 Farm Lane, Room 207. East Lansing, MI 48824. (steine84@msu.edu)

Tyrone O. Rooney: Michigan State University; 288 Farm Lane, Room 207. East Lansing, MI 48824. (rooneyt@msu.edu)

Guillaume Girard: Northern Illinois University; Davis Hall 312, Normal Rd. DeKalb, IL 60115 (ggirard@niu.edu)

Nick Rogers: School of Environment, Earth and Ecosystem Sciences, The Open University; Walton Hall, Milton Keynes. MK7 6AA, UK. (nick.rogers@open.ac.uk)

Cynthia Ebinger: Earth and Environmental Sciences, Tulane University of Louisiana, New Orleans, LA, USA. (cebinger@tulane.edu)

Liam Peterson: Michigan State University; 288 Farm Lane, Room 207. East Lansing, MI 48824. (ldpete@umd.edu)

Rayn Phillips: Michigan State University; 288 Farm Lane, Room 207. East Lansing, MI 48824. (phill782@msu.edu)

Abstract

The initial interaction between material rising from the African Large Low Shear Velocity Province and the African lithosphere manifests as the Eocene continental large igneous province (LIP), centered on southern Ethiopia and northern Kenya. Here we present a geographically well-distributed geochemical dataset comprising the flood basalt lavas of the Eocene continental LIP to refine the regional volcano-stratigraphy into three distinct magmatic units: (1) the highly-alkaline small-volume Akobo Basalts (49.4 -46.6 Ma), representing the initial phase of flood basalt volcanism derived from the melting of lithospheric-mantle metasomes, (2) the primitive and spatially restricted Amaro Basalts (45.2-39.58 Ma) representing the early main phase of flood basalt volcanism derived from the melting of the upwelling thermochemical anomaly, and (3) the spatially extensive Gamo-Makonnen magmatic unit (38-28 Ma) representing the mature main phase of flood basalt volcanism that has undergone significant processing within the lithosphere resulting in relatively homogeneous compositions. The focused intrusion of these main phase magmas over 10 m.y. preconditioned the African lithosphere for the localization of strain during subsequent episodes of lithospheric stretching. The focusing of strain into the region occupied by this continental LIP may have contributed to the initial extension in SW Ethiopia associated with the East African Rift.

Keywords: flood basalt, Ethiopia, magma plumbing system, magma recharge

Introduction

Continental large igneous provinces (LIPs), which are among the largest magmatic events on Earth, rarely record lava compositions that can be considered primary (Cox, 1980; Villiger et al., 2004). Such an observation requires residence and differentiation of magmas within the lithosphere evidenced by voluminous crystal cumulates within numerous intrusive complexes (Charlier et al., 2015). The impacts of such processes are profound: (a) significant volumes of dense material fractionated from transient magmas may greatly alter the bulk composition, hydration state, and thermal state of the continental crust, as well as contribute to the formation of structures such as High Velocity Lower Crust, all of which have uncertain feedbacks on rheology and continental rifting (Farnetani et al., 1996; Larsen et al., 2018; Montési, 2013; Ridley and Richards, 2010; Thybo and Artemieva, 2013); (b) the structure of a magmatic plumbing system may impact how magma degasses and over what timescales, with implications for climate change caused by such events (Self et al., 2005); (c) LIP plumbing systems are recognized as the host of significant economic mineral deposits such as Noril'sk-Talanakh beneath the Siberian LIP and those of the Duluth Complex associated with the Keweenawan LIP of North America (Naldrett, 2010). It is therefore apparent that resolving the processes contributing to the development of a magmatic plumbing system within a LIP has application beyond igneous systems to strain localization within continental interiors and exploration for economic mineral deposits.

The plumbing systems of LIPs must transmit large volumes of magma through the lithosphere in a relatively short interval (Jerram and Widdowson, 2005; Self et al., 1997). This assertion is supported by observations of large economic deposits that formed within LIPs where the volume of silicate magma required to create the deposit far exceeds the volume of the host intrusion (e.g. Eagle Mine, Michigan; Ding et al., 2012). The necessity for a high flux of magma through the magmatic plumbing system requires an interconnected system that is efficient at storing, transporting, and hybridizing magmas (Griselin et al., 1997; Jean et al., 2013; Lassiter et al., 1995; Lightfoot et al., 1990; Peng et al., 1994; Yu et al., 2015). LIP's lava compositions are therefore defined by an aggregate of processes, and are not limited to fractional crystallization and assimilation (e.g. Lee et al., 2014). Many continental LIPs exhibit lava compositions that are remarkably homogeneous with little variation from flow to flow in terms of major elements, although trace elements may exhibit more variability. Lava compositions show that major and trace elements appear to have decoupled from trends typically observed during fractional crystallization (Cox, 1980; Kieffer et al., 2004; Paces, 1990; Villiger et al., 2004). Probing the magmatic plumbing system of LIPs using such lava compositions thus requires the application of recharge-evacuation-assimilation-fractional crystallization (REAFC) models (e.g. Bohrson et al., 2014; Lee et al., 2014; Nishimura, 2019).

Continental LIPs are frequently highly eroded and dissected, with poor preservation of erupted sequences, which make probing their magmatic plumbing systems challenging (Ernst, 2014). Among the best-preserved LIPs is the Ethiopian-Arabian Large Igneous Province, which is dominated by distinct Eocene and Oligocene continental flood basalt provinces or continental LIP events. Among these two events, the Oligocene Ethiopian continental LIP, which coincided with the initial opening of the southern Red Sea rift at 30 Ma, has been the focus of more intensive study. Advancements in the understanding of the magmatic plumbing system within the Oligocene continental LIP has come from detailed petro-stratigraphic studies of flow-by-flow lava sequences (Kieffer et al., 2004; Krans et al., 2018; Pik et al., 1999), and their emplacement with respect to initial rift opening (Ukstins et al., 2002; Wolfenden et al., 2005). Trace element and isotopic studies have further shown that the Oligocene continental LIP is likely the result of an interaction of a mantle plume with the African lithosphere (Beccaluva et al., 2009; Kieffer et al., 2004; Natali et al., 2016; Pik et al., 1999). However, the Oligocene continental LIP was not the first manifestation of Cenozoic magmatic activity in East Africa. A thick sequence of stratiform primarily mafic lavas erupted in

southern Ethiopia and northern Kenya approximately 15 m.y. prior to the Oligocene continental LIP, roughly synchronous with the intrusion of kimberlites in central Africa (Ebinger et al., 2017). The relative paucity of parallel studies upon this Eocene continental LIP (Ebinger et al., 1993; George et al., 1998; George and Rogers, 2002; Stewart and Rogers, 1996) is due, in part, to difficulties with access to the region. With the recognition that the Eocene continental LIP represents approximately 25% of magmatism within the broader Ethiopian-Arabian LIP (Ebinger et al., 1993; Rooney, 2017), there is a need to examine the origin of the Eocene event and establish its relationship to the subsequent Oligocene continental LIP, as well as plateau uplift and strain localization as rifting initiated in East Africa (e.g. Kounidis et al., 2021; Faccenna et al., 2019; Pik et al., 2008).

Here we present a geochemical study of the Eocene continental LIP utilizing samples collected during the original mapping of the region in the 1970s (Davidson et al., 1973; Davidson, 1983). This sample suite allows for the most complete geochemical examination of the Eocene continental LIP to date. Through major and trace element characterization of these lavas, we find remarkable homogeneity in lava compositions erupted over a wide area. Using existing volcano-stratigraphy, we show that the majority of flood basalt lavas of the Eocene continental LIP, including the heretofore enigmatic "Makonnen Basalts" (Davidson, 1983; Rooney, 2017), share a common composition consistent with the Gamo Basalt unit (George and Rogers, 2002). We show that the broad geographic distribution of this relatively homogenous basaltic composition is consistent with the main phase of flood basalt activity within the Eocene continental LIP. We present an REAFC model constraining the magmatic system during the main phase of LIP volcanism that allows erupted lava compositions to be derived from a common primitive magma. The period over which the common primitive magma must have been recharging the REAFC system is considerably longer than a typical continental LIP. We assess the impact of this long-lived magmatic system on the thermal and compositional state of the crust and examine the implications for subsequent rifting of the African continent.

Background

Regional Overview

Holocene-recent magmatism associated with the East African Rift system south of the Red Sea is typically of limited areal extent and generally is restricted to rift basins and uplifted rift flanks, both onshore and in the Indian Ocean (Corti et al., 2019; Ebinger, 2020). Geophysical studies of the East African mantle reveal a seismic low-velocity zone above a mantle transition zone of relatively uniform thickness and broad distribution (Reed et al., 2016; Thompson et al., 2015). Such observations are interpreted as the upwelling of chemically distinct, volatile-rich material (Reed et al., 2016; Thompson et al., 2015) consistent with a mantle plume, however the geometry of the upwelling plume material is not well-defined and might not be representative of its geometry throughout Cenozoic (e.g., Boyce et al., 2021; Chang et al., 2020). Ambient noise and surface wave tomography, receiver function analyses, and limited controlled source seismic studies, with different techniques imaging the top and bottom of the accreted magmatic material, indicate that the crust beneath the Ethiopian plateau has been extensively underplated by mafic intrusions (e.g. Kounidis et al., 2021; Chambers et al., 2019; Lavayssière et al., 2018). Estimates of lithospheric thickness from surface wave tomography and mantle xenolith data are 100-88 km, respectively, suggesting moderate thinning of Pan-African lithosphere associated with heating and subsequent stretching (Priestley et al., 2008). These studies indicate that a profound degree of modification of the East African crust and mantle must have occurred prior to the onset modern magmatism.

A rich geochronological and geochemical framework has demonstrated that magmatism in East Africa has been both more volumetrically significant and more widely distributed than would be assumed from studies of modern magmatism (Baker et al., 1971; Brotzu et al., 1984; Brown and McDougall, 2011; Davidson et al., 1973; Ebinger et al., 1993; Furman et al., 2006; Guth, 2013; Hackman et al., 1990; Hofmann et al., 1997; Key and Watkins, 1988; Kieffer et al., 2004; Morley et al., 1992; Natali et al., 2013; WoldeGabriel et al., 1991). Using these studies, a recent synthesis has identified specific pulses of widespread basaltic magmatism at ca. 4 Ma, 10-12 Ma, and 20-26 Ma in the rift system East of the Tanzania craton (Rooney, 2020a, 2020b, 2020c). Each discrete magmatic pulse is linked with an extensional episode, providing a decompression melting mechanism for magma generation (Rooney, 2020b), however the volume of material erupted is suggestive of persistent elevated mantle potential temperature of the East African upper mantle (Armitage et al., 2015; Ferguson et al., 2013; Rooney et al., 2012). The most voluminous and widely distributed Cenozoic magmatic events in East Africa pre-date these pulses and occur during the Eocene and Oligocene (Abbate et al., 2014; Baker et al., 1996; Ebinger et al., 1993; George et al., 1998; George and Rogers, 2002; Hofmann et al., 1997; Pik et al., 1998; Rochette et al., 1998; Rooney, 2017; Ukstins et al., 2002). The flood basalt sequences of the Eocene and Oligocene continental LIPs record the most anomalous mantle potential temperatures and have geochemical signatures consistent with a derivation from the lower mantle (Pik et al., 1999; Rooney et al., 2012). It is therefore apparent that studies of the initial magmatic events provide insight into the long-term thermo-chemical perturbation of the East African upper mantle, with relevance to modern studies of melt generation within the East African Rift.

Existing stratigraphic and temporal constraints for the SW Ethiopian and northern E African Plateaus

Exposures of flood basalt sequences are facilitated by the ~18 Ma-Recent normal faulting and flank uplift across the region, which was accompanied by much smaller volume magmatism localized to the faulted rift valleys (Ebinger et al., 2000; Morley et al., 1992; WoldeGabriel et al., 1991). Paleaogene extension west of Lake Turkana remains enigmatic, and includes inversion of Mesozoic rift basins (Morley et al., 1999b, 1999a). The existing nomenclature for describing volcanic rocks of Eocene and Early Oligocene age in SW Ethiopia has not been standardized in the literature. Prior studies have used the terminology of a 'Pre-Rift Sequence' to refer to the flood basalt activity and related magmatic events in SW Ethiopia between ca. 50-28 Ma (Davidson and Rex, 1980; Davidson, 1983; George and Rogers, 2002). The 'Pre-Rift Sequence' represents several hundred to over 1500 meters stratigraphic section, composed of dominantly stratiform mafic lavas with silicic intercalations that increase in frequency towards the upper flows (Davidson, 1983). Widely mapped sub-divisions were originally recognized on the basis of petrographic characteristics, and later K-Ar isotopic age determinations as: (1) The Akobo Basalts (49.4 ±1.9 Ma to 46.6 ±2.0 Ma); (2) The Main Series (42.7±2.0 Ma to 32.7 ±1.3 Ma); and (3) The Makonnen Basalt (34.8 ±1.3 to 28.8 ±1 Ma) (Davidson, 1983). The Ethiopian Geological Survey has continued to use the mapped distribution of Eocene-Oligocene rocks as determined by Davidson (1983), but chose to reassign those units into a broader context. The Akobo Basalts, lowest in the Davidson section, were correlated to the Ashangi formation of the Oligocene continental LIP (Tefera et al., 1996). The overlying Main Series was transformed into the Jimma Volcanics, featuring a lower basaltic and upper mostly silicic unit, which covers most of the southern Ethiopian highlands. The Makonnen Basalts of Davidson (1983) were redefined and expanded to include all basalts of Oligocene age in SW Ethiopia that lie upon crystalline basement rocks (Tefera et al., 1996). Subsequent examination of the correlative ages between the Makonnen Basalts (~34.8-28.1 Ma) and the Oligocene continental LIP (~32-27 Ma) led Rooney (2017) to

hypothesize a link between the two, noting that additional geochemical and geochronological work was required to confirm this hypothesis.

The Eocene Amaro and Gamo Basalts of southern Ethiopia existing stratigraphic and temporal constraints

Several sections of stratiform basalts are exposed along the flanks of the Southern Main Ethiopian Rift and the rift basins of SW Ethiopia and northern Kenya that are contemporaneous with the 'Pre-Rift Sequence' of the SW Ethiopian Plateau (Figure 1). Unlike the 'Pre-Rift sequence', which was a broad regional compilation, these sections of stratiform basalts were examined using detailed stratigraphic, geochronologic, and geochemical techniques (Ebinger et al., 2000, 1993; George et al., 1998; George and Rogers, 2002; Stewart and Rogers, 1996). The type-sections for these lavas are in the Amaro region, but additional exposures are found west of the Gidole Highlands (GH, Figure 1). Initially recognized as Eocene in age (WoldeGabriel et al., 1991; Yemane and Yohunie, 1987; Zanettin, 1978), the sequence consists of two units that are distinctive in their petrographic character: (A) The lower Amaro Basalt, which erupted as much as 250 m of stratiform basalt over a red basal sandstone. Predominantly porphyritic, the Amaro Basalts commonly contain both olivine and plagioclase phenocrysts with rare clinopyroxene, consistent with a tholeiitic fractionation sequence (George and Rogers, 2002); (B) After a short hiatus in basaltic volcanism, locally marked by the silicic Arba Minch Tuff, there is a shift in petrologic character to marginally more evolved compositions with the eruption of the Gamo Basalts (Ebinger et al., 1993). Petrologically distinct from the underlying Amaro Basalt unit, the Gamo Basalt lavas are typically aphyric to weakly olivine porphyritic and generally more alkaline in composition.

Subsequent refinement of the temporal constraints of the Eocene continental LIP came from $^{40}Ar/^{39}Ar$ techniques, whereby a temporal break between an older Amaro Basalt and younger Gamo Basalt was recognized. The Amaro Basalt lavas exhibit a range in ages from 45.2 (±1.4) to 39.8 (±0.8) Ma (Ebinger et al., 1993; George et al., 1998). The Gamo Basalts (39.8 ± 0.6 Ma to 34.1 ± 0.5 Ma) are capped by the 33 Ma Amaro Tuff that blankets much of the Eocene-early Oligocene geologic section in SW Ethiopia (Davidson, 1983; Ebinger et al., 1993).

The relationship between the two established stratigraphic frameworks (i.e. 'Pre-Rift Sequence' and Amaro-Gamo Basalts) is ambiguous. While there are clear temporal similarities between the sequences, the lack of geochemical constraints from lavas in SW Ethiopia created difficulties in correlating flood basalt stratigraphy across the multiple magmatic basins that developed after eruption (Davidson et al., 1976; Ebinger et al., 2000). A notable overlap between the sequences is evident: Ebinger et al. (2000) correlated the widespread stratigraphic occurrence of stratiform basalts being overlain by a thick silicic tuff from a large eruption of an unknown volcano thereby expanding the Amaro-Gamo Basalts classification west of the Gidole Highlands (Figure 1) into regions mapped by Davidson (1983). The silicic tuff was interpreted by Ebinger et al. (2000) to be the Amaro Tuff and inferred the underlying lavas to be the Gamo Basalts. Further examination of the 'Pre-Rift Sequence' lavas from a geochemical perspective can help to confirm the hypothesis of Ebinger et al. (2000) and further expand this designation into the remainder of SW Ethiopia.

Stratiform Basalts in northern Kenya

The Turkana region of northern Kenya encompasses multiple exposures of stratiform mafic lavas that are contemporaneous with those in southern and southwestern Ethiopia (Brown and McDougall, 2011; Davidson, 1983; Furman et al., 2006; McDougall and Watkins, 2006; WoldeGabriel et al.,

1991; Zanettin et al., 1983). A recent synthesis of East African Rift magmatism (Rooney, 2017) tentatively divides the stratiform lavas of the Turkana region into the regional magmatic pulses of the Eocene Initial and Oligocene Traps phases. The Eocene initial phase in Turkana begins with the eruption the Balsea Koromto basalts (39.2-35.2 Ma; Furman et al., 2006; Wilkinson, 1988) in the Kajong region. Also included in the Eocene Initial Phase are the Nabwal formation (34.3 Ma; McDougall and Watkins, 2006) and Turkana Volcanics near Lokitaung town (31.1-36 Ma; Bellieni et al., 1981; McDougall and Brown, 2009; Morley et al., 1992; Tiercelin et al., 2012) (LK, Figure 1). Mafic lavas tentatively attributed to the Oligocene Traps phase outcrop on the perimeter of the Lotikipi Basin (Rooney, 2017; Wescott 1999, Brown and Jicha 2016; Brown and Mcdougall, 2011). The assignation of these lavas to the Oligocene Traps phase was based upon age determinations of silicic volcanics (32.5-31.7 Ma; Brown and Jicha, 2016) that overlie the stratiform mafic lavas. Seismic reflection surveys in western Turkana support the possibility that the stratiform lavas surrounding the Lotikipi basin may be correlative to those near Lokitaung town (Morley et al., 1999b; Wescott et al., 1999) (Figure 1).

While there is clear temporal correlation between the stratiform lavas in southern/southwestern Ethiopia and those in Turkana, the paucity of geochemical data prevents a robust conclusion of their relationship. The Turkana Volcanics at Lokitaung and the Nabwal formation are near the border with Ethiopia (Figure 1) making a correlation with the Amaro-Gamo sequence possible, though, existing geochemical information is limited to major elements (Bellieni et al., 1986; Tiercelin et al., 2012). Extant trace element geochemical studies in Turkana from this time period focused upon the Balsea Koromto (Furman 2006) that have a distinctive trace element signature inconsistent with existing lavas from southern Ethiopia. However, the Balsea Koromto lavas near Kajong are more than 150km farther southeast than the Turkana Volcanics (KJ, Figure 1.), making geographically broad interpretations on the relationship of contemporaneous lavas in Turkana with those in Ethiopia difficult. Additional geochemical data from the Turkana Volcanics can help to contextualize the Turkana stratiform lava's connection to the Eocene continental LIP lavas erupted in southern Ethiopia.

Methods

In order to compare lavas of the 'Pre-Rift Sequence' and the Amaro/Gamo Basalt division, we have undertaken a modern geochemical study of previously collected samples. The 'Pre-Rift Sequence' is represented by The Omo River Project sample suite (Davidson, 1983). Samples of this suite were collected between 1972 and 1974 during a collaborative Ethiopian Geological Survey- Geological Survey of Canada expedition to formerly inaccessible areas of SW Ethiopia between 4° and 8°N. In this study we have utilized thin section off-cuts loaned from the Geological Survey of Canada. We have re-created the sample catalog from original archive documentation and linked the sample numbers to location information provided at the time of sample collection. Given the collection period pre-dates GPS, the sample coordinates are those of 'stations' from the original catalog that were located by aerial photography (Figure 1). All metadata associated with this sample suite is linked to its IGSN catalogue number.

The small size of the remnant material available for study and need for sample archiving required geochemical analysis to be performed with in-situ analytical methods. Their relatively low crystallinity allows the use of a wide beam laser-ablation (LA)-ICP-MS technique as a proxy for bulk rock analyses. A total of 34 samples were trimmed, and fragments were mounted in 25mm epoxy molds and polished. The polished sample fragments were analysed simultaneously by LA-ICP-MS for major and trace elements using a 15x15 cm two-volume cell-equipped Teledyne Photon Machines

Analyte G2 excimer laser coupled to a Thermo Scientific ICAP Q ICP-MS at Michigan State University. Given the assumed inhomogeneity of the samples, fifteen, 1mm long by 150 μm wide surface ablation scans were collected from each sample in order to obtain a representative geochemical characterization. The 15 scans from each sample were then scrutinized statistically, using the following methodology, to ensure they were representative of a "whole rock" composition. Standard deviations were calculated from each sample's 15 scans. Those individual scans whose compositions fell out of 5% relative standard deviation of their sample average composition were considered suspect and reviewed in the microscope. If the same scan was determined to have intersected a non-representative amount of crystal phases it was omitted from the average composition calculation and is not reported in this study. Out of 310 line-scans a total of eight were identified as problematic and removed from their respective sample averages. Further details on standard reference materials and their reproducibility, and the validated data can be found in the supplemental materials.

The geochemical data for the Omo River Project suite collected using the method discussed above are broadly comparable to conventional whole-rock powder techniques, evidenced by the overlap in X-Y variation diagrams with data from Amaro-Gamo Basalts and the Oligocene continental LIP (supplementary X-Y plots). Our new raster line data does deviate from the regional dataset, clustering lower concentrations of TiO_2 and Al_2O_3 but remains within the overall spread of existing data. Importantly, despite minor shifts in select major elements, trace elements abundances and spider diagram patterns (Figures 3 and 4) are comparable to whole-rock analyses of contemporary lavas in southern Ethiopia and northern Kenya. Given the similarity of these analyses to regional geochemical data it is evident that data collected using this novel method are consistent with data collected by standard whole-rock methods. The Amaro-Gamo Basalts units have previously been examined for major and trace elements (George and Rogers, 2002; Stewart and Rogers, 1996). These previous studies determined major and trace element abundances through combined XRF and INAA techniques, with a subset of samples analysed by more precise ICP-MS methods. Here we present new whole-rock ICP-MS data for a total of 20 samples that were re-analysed for 38 trace elements at Open University using techniques described in Rogers et al. (2006).

To expand the spatial distribution of the known Eocene-Oligocene sample suite from Southern Ethiopia, we collected new whole-rock major and trace element data from a suite of samples acquired during several sampling campaigns to the Yerer Tullu-Wellel Volcanic Lineament (3096 and 3098), Southern Main Ethiopian Rift (3124, 3125, 3126, 3152 and 3153), and Lokitaung, Kenya (TOR0000NO, collected by Dr. Frank Brown). Samples were cut, polished to remove saw marks, and cleaned in an ultrasonic bath before crushing in a steel jaw crusher. Crushed material was powered in a Bico ceramic disk mill. Dried powers were then mixed with Li-Tetraborate flux and fused into glass disks following procedures detailed in Rooney et al., (2011). Major element analysis of fused disks was performed on a Bruker S4 Pioneer XRF spectrometer. Trace element concentrations were collected on these same disks by LA-ICP-MS using the apparatus described above, following procedures of Rooney et al. (2015). Detailed information of standards and analytical replicates for XRF and ICP-MS analyses can be found in supplemental documents.

Results

Overview of Geochemical Results

Geochemical data from this study can be divided, based on whole rock major element compositions, into two coherent lava groups: (1) a transitional to alkaline population (basalt to trachybasalt) constituting the majority of the dataset, and (2) a smaller population of tholeiitic basalts (Le Maitre,

1989). Alkaline samples are commonly more evolved (4-6 wt. % MgO) and exhibit high TiO_2 and Zr. The tholeiitic basalt sub-group is generally more primitive (6.5-10 wt. % MgO) and is consistently less enriched in TiO_2 and Zr than the alkaline samples. Trace element patterns show similar behavior among the datasets: most samples exhibit a convex upward primitive mantle normalised pattern with variability in incompatible trace element enrichment (Figure 3). To a first order, incompatible trace element profiles reflect the major elements and split the dataset into two groups: a dominantly tholeiitic group and a dominantly alkaline group. The tholeiitic group (Amaro Basalts) has a depleted and flatter profile in both primitive mantle normalised and chondrite normalised REE diagrams. The dominantly alkaline group (Gamo Basalts, Akobo Basalts, Main Series, Makonnen Basalts, Turkana Volcanics) has more enriched incompatible trace elements in primitive mantle normalised diagrams and steeper profile in chondrite normalised REE diagrams.

Southern Ethiopia: Amaro – Gamo Basalts

Amaro Basalts

Our new data on the Amaro and Gamo Basalts clarify and expand the geochemical patterns previously established. Consistent with this model, the tholeiitic Amaro basalts exhibit more primitive compositions with higher MgO (~7-11 wt. %) and a marked depletion in the most incompatible trace elements in comparison to other units from SW Ethiopia. This depletion is evident in the chondrite normalised pattern (Figure 4), showing a relatively flat slope in the LREE, and HREE: $(La/Sm)_{CN}$ = 1.2-2.0, and $(Tb/Yb)_{CN}$ = 1.3-2.0. Amaro Basalt samples plot within the depleted domain, defined in terms of elevated Zr/Nb and low La/Yb values (Figure 2). The primitive mantle normalised pattern of the Amaro Basalts is dominated by the superimposed, pronounced positive anomalies in certain LILE (e.g. Ba) over the generally depleted composition of the other incompatible trace elements (Figure 3). On the basis of these primitive mantle normalised patterns, Amaro Basalt lavas classify as Group Ib based upon the collation of Rooney (2017).

Gamo Basalts

Consistent with the established Amaro-Gamo Basalt geochemical framework, the alkaline Gamo Basalts exhibit modestly evolved compositions with lower MgO (4-6 wt. %) and enriched trace element characteristics. Modest enrichment is visible in chondrite normalised diagrams where the Gamo Basalts have a flat profile that is steeper than the Amaro basalt $(La/Sm)_{CN}$=2.2-2.5 and $(Tb/Yb)_{CN}$=1.6-2.1). The Gamo Basalts plot near the Amaro Basalts in Zr/Nb vs. La/Yb, but are displaced to more enriched values (Figure 2). Primitive mantle normalised diagrams show a convex upward pattern, with positive Ba and Pb, and negative K anomalies (Figure 3). Internal variation within the Gamo Basalt dataset is small, evidenced by the narrow range between the 1st and 3rd quartiles in Figure 3. Rooney (2017) noted that the Gamo Basalt lavas are not entirely consistent with the Type Ib magma group due to the enrichment in trace elements, a feature common to the Type III magma group.

Southwestern Ethiopia: Stratiform Basalts of the Omo Region

Akobo Basalt

Trace element behavior for the strongly alkaline Akobo Basalt is unlike other Eocene magmatic units in SW Ethiopia due to its strong enrichment in incompatible trace elements. The Akobo Basalts exhibit a steep REE profile (Figure 4) displacing the $(Tb/Yb)_{CN}$-$(La/Sm)_{CN}$ ratio to values near the Turkana Eocene field of Furman et al. (2006) (Figure 2). Similar behavior is noted in Zr/Nb-La/Yb

space where the Akobo Basalts plot toward the Turkana Eocene lavas and a more enriched domain (Figure 2). Primitive mantle normalised patterns show enrichment in the incompatible elements and depletion in K but lack the distinctive Ba and Pb of the Amaro-Gamo Basalt units (Figure 3). The Akobo Basalt trace element patterns classify as a Type II magma (Rooney, 2017), similar to the HT2 Oligocene flood basalts (Beccaluva et al., 2009; Natali et al., 2016; Pik et al., 1999) and lithosphere-derived lavas from Kenya and Ethiopia (Rooney, 2020b).

Main Series

Most of the Main Series samples are transitional to alkaline in composition (Figure 2) and show evidence of being evolved: 4-6 wt. % MgO and 2.5-4 wt. % TiO_2. Trace elements in these Main Series samples exhibit more enriched characteristics consistent with the Gamo Basalts, evident in the greater slope of the REEs $(La/Sm)_{CN}$=1.5-8 and $(Tb/Yb)_{CN}$=1-2.1). Chondrite normalised REE diagrams show a weak negative Eu anomaly (Figure 3) on an otherwise flat pattern. These data plot in La/Yb versus Zr/Nb toward more enriched values, overlapping with data from the Gamo Basalts (Figure 2). Primitive mantle normalised diagrams show these Main Series data exhibit a modestly enriched pattern, with positive anomalies in Ba and Pb similar to patterns of the Gamo Basalts. As with the Gamo Basalts, this pattern does not comport with the magma type grouping of Rooney (2017). When examined with the 1st and 3rd quartiles for the distribution of data for known Gamo Basalt samples, it is apparent that the Main Series and Gamo Basalts share the same geochemical signature. Given the similarities between the Main Series lavas and the Gamo Basalts, we hereby assign most of the Main Series samples to the Gamo Basalt.

The samples classified as the Main Series are dominantly transitional to alkaline in composition, except for a subset of samples that are sub-alkaline (Figure 2). The two sub-alkaline samples (TOR0000GG and TOR0000H9) appear somewhat more primitive, plotting at greater concentrations of MgO wt. % and lower TiO_2 and P_2O_5. These data show depleted trace element characteristics as evidenced by the shallow slope through the REEs (Figure 4) and low values of $(La/Sm)_{CN}$ (Figure 2). Similar behavior is observed in Zr/Nb versus La/Yb where these two samples plot toward more depleted values. Trace element patterns in primitive mantle normalised diagrams exhibit positive anomalies in Ba and Pb superimposed on a broadly depleted convex upward pattern (Figure 3). Such characteristics are consistent with Type Ib magmas of Rooney (2017) and LT magmas (Kieffer et al., 2004; Pik et al., 1999, 1998). The data from these two samples consistently plot near the Amaro Basalts in X-Y variation diagrams and are sub-parallel with the Amaro Basalt trace element patterns detailed above. Therefore, we assign these two samples to the Amaro Basalt unit characterized geochemically by previous studies (George and Rogers, 2002).

Makonnen Basalt

The data for the Makonnen Basalts are transitional to alkaline in composition (Figure 2), have MgO between 4.5 and 6 wt. % and generally resemble the Gamo basalts. Variation diagrams versus MgO show the Makonnen Basalts overlap with data from the Gamo Basalts (e.g. CaO, and P_2O_5), while trace element data for these samples indicate modest enrichment in La/Yb versus Zr/Nb and an REE slope within the range of the Gamo Basalts $((La/Sm)_{CN}$ =2.1-2.9 versus $(Tb/Yb)_{CN}$=1.4-1.7). Trace elements normalised to primitive mantle are similar to those defined by the 1st and 3rd quartile of the Gamo Basalt data, showing a convex upward pattern with modest enrichment in the incompatible trace elements and superimposed positive Ba and Pb anomalies (Figure 3). Given the similarities between the Makonnen Basalts and the Gamo Basalts, the two are considered to be the same magmatic unit that we define as the Gamo-Makonnen magmatic unit (Figure 5).

Turkana Volcanics near Lokitaung

A single sample of the Turkana Volcanics near Lokitaung was analyzed for major and trace elements (TOR0000NO). This sample is a transitional basalt that contains 4.5% MgO and 2.9 % TiO_2 indicating a moderate degree of evolution. Trace element data indicate moderate enrichment in La/Yb versus Zr/Nb and REE element slope comparable to the Gamo Basalts $(La/Sm)_{CN}$ =2.6 versus $(Tb/Yb)_{CN}$=1.4. Primitive mantle normalised patterns (Sun and Mcdonough 1989; Figure 3) for the Turkana Volcanics are parallel to, and within the 1st-3rd quartile range for the Gamo Basalts. Due the similarity in geochemical characteristics between the Gamo Basalt and the Turkana Volcanics, we tentatively assign the Turkana Volcanics to the Gamo-Makonnen magmatic unit with the caveat that this assignation is based upon a single analysis and requires further study to confirm the relationship.

Discussion

The regional scale geochemical dataset presented here permits a synthesis of the two systems by which Paleaogene volcanic rocks of southern and SW Ethiopia are described, and it provides tentative links to NW Kenya stratigraphic sequences. The existing country-scale map of Ethiopia utilizes a stratigraphic sequence for the Eocene units of SW Ethiopia based upon regional scale mapping and geochronology, dominantly undertaken by The Omo River Project surveys during the 1970s (Davidson and Rex, 1980; Davidson, 1983). Subsequent and more detailed mapping, geochemical characterization, and precise $^{40}Ar/^{39}Ar$ geochronology of discrete volcano-stratigraphic sections established an alternate stratigraphy based upon the Amaro Basalt and Gamo Basalt units (Ebinger et al., 1993; George et al., 1998). The resolution of these two schemes into a unified volcano-stratigraphic sequence (Figure 5) has heretofore not been possible due to a lack of regional-scale geochemical characterization of the lavas in SW Ethiopia.

The newly resolved volcano stratigraphy in southern and SW Ethiopia allows for the interpretation of magmatic processes within the poorly characterized Eocene continental LIP. We expand upon the work of George and Rogers (2002) in the Amaro-Gamo region and explore the origin of the remarkable homogeneity in erupted lava compositions that are found throughout the region and persist for ~10 Ma. While the duration of volcanism does extend into the Oligocene, we utilize the term Eocene continental LIP to reflect the onset of this magmatic pulse, Eocene Initial Phase, as defined by Rooney (2017). We examine the impact of persistent and voluminous magmas staging within the crust by assessing the thermal and compositional state of the crust as a prelude to rift development. We interpret these observations within a developing paradigm of an East African upper mantle that is more complicated, both thermally and compositionally, than can be accommodated by the mantle plume head-tail model (e.g., Pik et al., 2006; Bastow et al., 2008; Chang and van der Lee, 2011; French and Romanowicz, 2015).

Unified Eocene Stratigraphy

Earliest Alkaline Magmatism (>45 Ma)

There is a growing recognition that pre-flood basalt small-volume alkaline magmatism may be more common in East Africa than initially considered. Instances of such activity are observed in the Oligocene continental LIP located on the NW Ethiopian Plateau, where Krans et al. (2018) identified a clinopyroxene-phyric alkaline basaltic sequence at the base of the Oligocene continental LIP. The Akobo Basalts, which occur at the base of the Eocene continental LIP flood basalt sequence, share a similar petrographic character and contain abundant large, strongly zoned titaniferous clinopyroxene

and olivine. We interpret these small volume alkaline events as representing the initial phase of flood basalt (LIP) volcanism, as defined in the tripartite division of Jerram and Widdowson (2005).

We show that the Akobo Basalts are the most silica-undersaturated lavas in the Eocene stratigraphy in SW Ethiopia (Figure 2), and exhibit a Type II lava pattern (Rooney, 2017). The Type II lava patterns evident in the Akobo Basalts suggest a likely origin within a metasomatized amphibole-bearing lithospheric mantle, which may have been thermo-barically destabilized by the Afar plume, and either melted in-situ or foundered into the upper mantle (Furman et al., 2016; Rooney et al., 2017, 2014). Broadly compositionally-equivalent magmatism is also evident at the southern edge of the Eocene continental LIP in Turkana (Kenya). The Balsea Kormoto (35-39 Ma; Furman et al., 2006) lavas are dominantly silica-undersaturated Type II lavas that are located East of Lake Turkana in the Kajong region (KJ, Figure 1). These lavas have been similarly interpreted as being derived from metasomatized lithospheric mantle (Furman et al., 2016; Rooney, 2017, 2010). The younger ages of these rocks suggests this style of magmatism may persist during the main flood basalt episode in more distal portions of the province.

Amaro Basalts (45-39 Ma)

Following the Akobo Basalts, ~ 250-300 m of moderately evolved stratiform basalts were erupted to form the Amaro Basalts. Prior studies have noted the prevalence of these Amaro Basalts in the region surrounding the Amaro horst, and constrained the eruption of the Amaro Basalts within a window of about 5 Ma (45.2-38.58 Ma; Ebinger et al., 1993; George et al., 1998). An important unknown in earlier studies has been the potential wider spatial distribution of the Amaro Basalt lavas than is currently understood. Prior to this study, the geochemical characterization necessary to assign lavas to the Amaro Basalts was limited to sections along the flanks of the Ethiopian Rift, extending as far west as the Mago Basin (Figure 1). We interpret these primitive lavas as representing the early stage of the main phase of flood basalt volcanism, as defined in the tripartite division of Jerram and Widdowson (2005).

The new dataset we present expands the spatial coverage of geochemically characterized lavas within the province (Figure 1). Previous nomenclature for these lavas assigned them to the undifferentiated 'Main Series' (~43-34 Ma) of the Pre-Rift Sequence (Davidson, 1983), which temporally occupies the same time window assigned to both the Amaro Basalts (45.2-39.58 Ma) and Gamo Basalts (38-34 Ma; Ebinger et al., 1993; George et al., 1998). Examination of the Main Series samples shows that lavas with Amaro-like compositions (Figure 3) are dominantly restricted in spatial distribution, focused on the region flanking the Ethiopian Rift (Figure 1). An important outcome of these observations is the confirmation that the locus of volcanism during the early stages of the flood basalt event is towards the Amaro horst (George and Rogers, 2002).

Gamo Basalts (38-34 Ma)

Following the eruption of the Amaro Basalts, there is a hiatus in basaltic volcanism that is represented by the Arba Minch tuff from an unknown volcanic centre (>39 Ma; Ebinger et al., 1993). Flood basalt volcanism (Gamo Basalts) recommenced with the eruption of a relatively more evolved suite of basaltic lavas and intercalated tuffs. The age range of the Gamo Basalts (38-34 Ma; Ebinger et al., 1993; George et al., 1998) overlaps the Main Series lavas (~43-34 Ma) of the 'Pre-Rift Sequence' (Davidson, 1983). Despite this temporal overlap, the genetic relationship between the two sequences has been unclear due to the lack of geochemical constraints on Main Series lavas. Our new results show that most Main Series lava samples geochemically resemble the Gamo Basalts. We therefore

assign the majority of the Main Series to the Gamo Basalts, thereby refining the previous *en masse* assignation of the Main Series to Amaro Basalt-Gamo Basalt Sequence (Rooney, 2017). This observation vastly improves the constraints on the spatial distribution of the Gamo Basalt unit, which are now shown to occupy much of the province and comprises up to 1500 m of lava flows and silicic volcaniclastics (Davidson, 1983; Rooney, 2017). The widespread distribution of silicic volcaniclastics erupted from unidentified volcanic centres (Amaro Tuff, Ebinger et al., 1993; Jvr unit, Tefera et al., 1996) was used by Ebinger et al. (2000) to suggest the Gamo basalts extended into SW Ethiopia. Our observations of similar geochemical characteristics between the Main Series of SW Ethiopia and the Gamo Basalts support the hypothesis of Ebinger et al. (2000).

Contemporaneous stratiform lavas in the Turkana region of northern Kenya (Figure 1) also exhibit Gamo Basalt-like geochemical characteristics. These lavas are represented in this study by a sample from the lower-most flows of the gorge east of Lokitaung town, estimated to be ~36 Ma (Brown and McDougall, 2011). This lava exhibits a primitive mantle normalised pattern nearly identical to that of the Gamo Basalt suite (Figure 3). Therefore, we tentatively assign the Lokitaung Basalts to the Gamo Basalt group and recognize that the limited geochemical data from Eocene-Oligocene lavas in the Turkana region prevents more robust conclusions. Additional geochemical characterization of the stratiform basalts in Turkana is required to fully evaluate the potential connection between those lavas and the neighboring Gamo Basalts.

Makonnen Basalts (34 – 28 Ma)

The Makonnen Basalts are the youngest stratigraphic unit associated with the 'Pre-Rift Sequence' of SW Ethiopia (Davidson, 1983). The prior stratigraphic separation of the Makonnen Basalts from the underlying Main Series (now Gamo Basalts) was the result of an angular unconformity between the two units (Davidson, 1983). This temporal break is reflected in the ca. 31.8 Ma average age determination for the Makonnen basalts, suggesting a younger age than much of the Main Series (Davidson and Rex, 1980) and Gamo Basalts (38-34 Ma; Ebinger et al., 1993; George et al., 1998). As with previous stratigraphic units within the 'Pre-Rift Sequence', the relationship between the Makonnen Basalts and the Amaro Basalt-Gamo Basalt Sequence has been unclear.

We have now shown that the Makonnen Basalts and the Gamo Basalts share a common geochemical signature and are hereby treated as a single magmatic unit (Gamo-Makonnen magmatic unit) for the purposes of exploring the magma genesis of the Eocene continental LIP. This amalgamation has implications for the distribution of Eocene continental LIP lavas in time and space. The Gamo-Makonnen grouping covers nearly the entire footprint of the Eocene continental LIP (Figure 1), making this group the most volumetrically significant unit in SW Ethiopia. Additionally, the Gamo-Makonnen unit occupies a broad time window, potentially extending from 38-28 Ma. We interpret these homogenous, relatively evolved lavas as representing the main phase of flood basalt volcanism, as defined in Jerram and Widdowson (2005). In the following discussion, we examine how homogenous lava compositions could be erupted over a broad spatial and temporal window through the examination of the magmatic processes impacting magma compositions during the Paleaogene in East Africa.

Lithospheric Modification of Magmas in the Eocene Province

Utilizing the newly established magmatic stratigraphy for the Eocene continental LIP, (Figure 5), it is now possible to examine the magmatic conditions present during the main phase of activity across the whole of the province (~320,000 km^2, Rooney, 2017). Prior work hypothesized that the Amaro Basalt and Gamo Basalt primary magmas are derived from sub-lithospheric reservoirs. Heterogeneity between the two primary magmas was thought to result from differential degrees of fractional crystallization of a primary magma (George and Rogers, 2002). With the recognition that recharge-

evacuation-assimilation-fractional crystallization (REAFC) processes may impose significant heterogeneity in the composition of lavas in continental LIPs (Paces, 1990; Turner et al., 1999; Yu et al., 2015), we explore the possibility that the Amaro and Gamo Basalts are derived from a common primary magma.

Melt Generation during the Eocene in Southern Ethiopia

The current model explaining the origin of the Eocene continental LIP focuses upon differing intensive parameters of melting and polybaric fractionation to generate lava compositions for the Amaro Basalt and Gamo-Makonnen units (George and Rogers, 2002). The melting conditions during the eruption of the Amaro Basalts were determined by George and Rogers (2002) to be consistent with experimental compositions derived by 3-7% fractional melting of the primitive mantle between 1.5-2 GPa at approximately 1480°C. Melt fractions decrease to ~2% during the eruption of the Gamo Basalts 5-10 m.y. later. As noted by George and Rogers (2002) the pressure and temperature of melting require an elevated mantle potential temperature beneath southern Ethiopia at the time of eruption, consistent with the presence of a mantle thermochemical anomaly during this time (Ebinger and Sleep, 1998; George et al., 1998; Rooney et al., 2012).

Conceptual model of the magmatic differentiation system in the Eocene Province

The primary compositional difference between the Amaro and Gamo Basalts units is thought to be imparted by their degree of differentiation. The Gamo Basalts are recognized as being more differentiated than the Amaro Basalts, an interpretation supported by the lower MgO (wt. %) and greater trace element abundances of the Gamo Basalts (George and Rogers, 2002; Stewart and Rogers, 1997). George and Rogers (2002) indicate that assimilation is not the primary agent of differentiation in the Amaro-Gamo magmatic system as it would require unreasonable amounts of assimilant to be incorporated given the bulk composition of the lavas. Additionally, a simple fractional crystallization sequence cannot be accommodated due to the seemingly contradictory petrographic observations and major element characteristics (George and Rogers, 2002). The Amaro and Gamo lavas are noted to contain gabbroic fractionation products that likely formed at shallow depths. However, compositional data indicate a correlation between MgO and the ratios of Sc/Yb and CaO/Al_2O_3 that is contradictory to evolution in a shallow magmatic system. Both ratios decrease with decreasing MgO, an observation consistent with deep fractionation of clinopyroxene (George and Rogers; 2002 and citations therein). MELTS models (Ghiorso and Sack 1995) similarly demonstrate the control of deep fractionation on Amaro-Gamo compositions which lie along the 0.5 GPa liquid line of descent (George and Rogers, 2002). The presence of plagioclase phenocrysts formed at shallow depths coupled with evidence of deep clinopyroxene fractionation led George and Rogers (2002) to conclude that the Amaro-Gamo Basalts evolved by polybaric differentiation pathways. The Amaro-Gamo primary magmas underwent deep fractionation of clinopyroxene and olivine prior to being released to higher crustal levels where gabbroic differentiation occurred forming the crystal cargo observed in the lavas.

Our new results based upon a series of observations of the Gamo-Makonnen magmatic unit are difficult to interpret within the existing magma genesis model for the Eocene-Oligocene lavas in southern Ethiopia. Firstly, our results show that the Gamo-Makonnen lavas are a single magmatic unit representing the large volume main phase of flood basalt volcanism that began in the Eocene and extended into the Oligocene. This observation is difficult to reconcile with the existing magma genesis model for the Eocene continental LIP that suggests the primary magma of the Gamo-Makonnen unit is generated by a smaller degree of mantle melting. Second, as noted by George and

Rogers (2002) and this study, the Gamo-Makonnen unit is remarkably homogenous in terms of major and trace element characteristics. It is unlikely, given the new broader spatial and temporal constraints on the Gamo-Makonnen magmatic unit, that fractional crystallization can account for the observed compositional homogeneity. The wide spatial distribution of the Gamo-Makonnen unit would require many closed magmatic systems evolving along an identical differentiation pathway. Additionally, the long temporal window occupied by the Gamo-Makonnen lavas requires these presumably identical magmatic systems to either: (1) evolve only to the composition of the erupted lavas and remain there for the duration of eruption, or (2) new magmatic systems must be formed that also follow the identical differentiation pathway. Additional processes must be active in the magmatic system of the Eocene continental LIP that can reconcile the differentiation pathway identified by George and Rogers (2002) and the broad spatial and temporal constraints from this contribution.

The magmatic systems of continental LIPs are long-lived and modify transient magma through several magmatic processes. Several lines of evidence support a largely open system, in contrast to isolated closed 'magma chamber' systems. While fractional crystallization is widely recognized as one of the primary processes contributing to magma differentiation, additional mechanisms including assimilation of crustal material play an important role (e.g. Bohrson and Spera, 2001; Spera and Bohrson, 2001). However, there is a growing recognition that the closed magma chamber model for differentiation may not accurately represent the large, high-flux magmatic systems of LIPS (Bohrson et al., 2020, 2006; Krans et al., 2018; Paces, 1990; Steiner and Streck, 2019; Streck and Grunder, 2012; Turner et al., 1999; Yu et al., 2015). The magmatic differentiation system of continental LIPs undergo episodic recharge and evacuation that results in hybridized magmas, whose evolutionary pathway is defined by the balance of recharge/evacuation and fractional crystallization/assimilation. For example, where fractional crystallization outpaces the recharge of magma into the system, the resultant lavas will progress toward more evolved compositions. During periods of high magma-recharge rates, the influx of new, primitive magma will drive lava compositions toward less evolved compositions, an effect not likely under closed-system differentiation. Furthermore, when recharge and crystal fractionation are balanced, the magmatic system reaches a steady or buffered state, erupting lavas whose composition remains constant over time. Critically, the buffering of individual elements is strongly dependent on their degree of compatibility, where compatible elements will quickly reach a buffered state while incompatible elements take longer (Lee et al., 2014). Lavas erupted from a buffered REAFC dominated system can exhibit significant enrichment and/or variability in incompatible trace elements abundances with limited variation in compatible elements (Lee et al., 2014). This subtle interplay between the REAFC components may explain the geochemical trends observed in the Eocene continental LIP.

Numerical modelling of magma differentiation in the Eocene Province

To probe the processes active within the Gamo-Makonnen magmatic system and to reveal constraints as to the potential flux of magma from the mantle, we undertook REAFC modeling of the Gamo-Makonnen magmatic system. To allow for efficient exploration of the model parameter space, we developed a Python implementation of the base equations for a constant mass box model developed by Lee et al. (2014). Our model examines REAFC, AFC, assimilation, and fractionation crystallization solutions over a range of evacuation, recharge, assimilation, and crystallization conditions. The primary model outcomes are liquid lines of descent representing each of these processes. For AFC, assimilation, and fractionation crystallization, these liquid lines of descent represent evolution of a single magma chamber without mass addition or subtraction. REAFC modelling requires a persistent magma chamber where mass is continuously added (recharged) or removed (evacuated). Lee et al. (2014) described a complete mass exchange within the magma chamber as an 'overturn'. Liquid lines of descent for REAFC models therefore represent the composition of the residual liquid that has been hybridized over potentially multiple overturns. As the

number of overturns increases, the REAFC solutions trend towards a steady state that is termed 'buffered'.

Conceptually, we explored whether the Gamo-Makonnen Basalts can be produced by REAFC modification from an Amaro Basalt composition. To that end, we presume the initial magma chamber composition and recharging magma composition is equivalent to a primitive Amaro Basalt lava. We do not utilize previously calculated primary Amaro Basalt compositions (George and Rogers, 2002) given the presumption that some olivine loss would occur in the lower crust, prior to entering the REAFC system. The assumed assimilant is an average middle crustal composition (Rudnick and Gao, 2003).

Fractional crystallization parameters were set to include crystallizing phases of olivine, clinopyroxene, plagioclase, and Fe-Ti oxides, reflective of those noted in petrographic descriptions and genetic models of previous studies (Davidson, 1983; George and Rogers, 2002). The examined range of modal abundances for crystallizing phases are as follows: olivine 0.22-0.8, clinopyroxene 0.15-0.5, plagioclase 0-0.3, while Fe-Ti oxides were held constant at 0.05 (where the proportion of Ilm/Mt = 9).

To examine the change in magma composition as a result of REAFC processes, we examined a suite of both compatible and incompatible elements that are sensitive to the crystallization specific phases or are indicative of assimilation. For the compatible elements we chose to examine MgO as a proxy for the degree of differentiation and Ni and Cr to probe the fractionation of mafic phases, whereby Ni and Cr partition into olivine or clinopyroxene, respectively. The behavior of incompatible elements was examined through: (1) Sr, which is affected primarily by the fractionation of plagioclase, (2) Nb, which is sensitive to Fe-Ti oxides or assimilation, and (3) La, which behaves incompatibly throughout the range of MgO concentrations examined by this study. Partition coefficients between minerals and basaltic liquid used by this study are described by: (Bougault and Hekinian, 1974; Ewart and Griffin, 1994; Green et al., 2000; McCallum and Charette, 1978; McKenzie and O'Nions, 1991; Nielsen et al., 1992; Paster et al., 1974; Ringwood and Essene, 1970).

The REAFC model presented here assumes the system is at constant-mass requiring equivalency of input (recharge and assimilation) and output (fractional crystallization and eruption) parameters. This constant mass assumption results in a hybrid parameter wherein there is a continuous balance between the degree of recharge and evacuation. Three REAFC parameters were examined over a range of values: (1) fractional crystallization, which varied from 20-98%, (2) eruption/recharge, which varied from 0-78%, and (3) assimilation, which varied from 0-15%. Within this parameter space, three solutions resulted in liquid lines of descent that bracket the cluster of data defined by Gamo-Makonnen composition.

The modelled liquid lines of descent for fractional crystallization, pure assimilation, and AFC fail to provide solutions that adequately reproduce the Gamo-Makonnen dataset. These solutions yield liquid lines of descent that contain an insufficient concentration of incompatible trace elements to pass through the Gamo-Makonnen dataset (Figure 6). In contrast, REAFC models do provide a sufficient enrichment in incompatible trace elements such that model curves pass through the observed data. However, a single initial/recharge magma composition cannot generate an array of curves that circumscribe the observed dataset.

An explanation for the failure of REAFC curves to circumscribe the data, despite significant leverage in model parameter variability, reflects an important principle of REAFC models – the potential to fractionate the behavior of elements based upon compatibility. Specifically, the degree of compatibility of any element within the fractionating phases impacts the point at which that element may become buffered and no longer vary with continued REAFC processing. Each element examined

reaches buffered conditions at different points during the evolution of the magmatic system. Compatible trace elements and MgO become buffered within three overturns, consequently, these elements rapidly reach steady state within the magma chamber. The results of our modelling illustrate the necessity for three different initial/recharge magma compositions to accommodate the observed compatible element characteristics. The rapid buffering of MgO prevents any single model solution from exhibiting a traditional liquid line of descent whereby MgO would fall with progressive melt evolution (Figure 6). Our REAFC model results instead reach a minimum buffered MgO value below which the magma compositions will not fall, irrespective of further differentiation within the magma system. These model outcomes have further implications for coupled variation in MgO versus incompatible trace element concentrations – notably it is possible to generate a wide range of incompatible trace element concentrations (and ratios) at common values of MgO from a single primitive magma composition. The implication of these observations is that the initial/recharge magma composition may vary within the Gamo-Makonnen magmatic unit.

Three solutions from our REAFC modelling bracket the majority of the Gamo-Makonnen data (Figure 6). The primary difference among these three solutions is the composition of the initial and recharging magma:

(1) Low MgO solution. The initial/recharge magma was ~8 wt. % MgO (sample RG93-73). The fractionating modal assemblage was: 0.22 olivine, 0.60 clinopyroxene, 0.13 plagioclase, 0.05 ilmenite+magnetite. REAFC parameters of fractional crystallization 90%, recharge 8%, assimilation 2%.

(2) Middle MgO solution. The initial/recharge magma was 10 wt. % MgO (sample RG93-75). The fractionating modal assemblage was: 0.32 olivine, 0.50 clinopyroxene, 0.13 plagioclase 0.05 ilmenite+magnetite. REAFC parameters of fractional crystallization 96%, recharge 2%, assimilation 2%.

(3) High MgO solution. The initial/recharge magma was ~11 wt. % MgO (sample RG93-74). The fractionating modal assemblage was: 0.32 olivine, 0.50 clinopyroxene, 0.13 plagioclase 0.05 ilmenite+magnetite. REAFC parameters of fractional crystallization 92%, recharge 6%, assimilation 2%.

While three distinctive initial/recharge magmas were required to capture the variance in the Gamo-Makonnen geochemical data, other model parameters (REAFC proportions, modal assemblage, etc..) did not vary significantly between solutions. The model parameters for all three best-fit solutions showed that fractional crystallization is the dominant process controlling the liquid lines of descent (90-96 %), while recharge/evacuation (2-8 %), and assimilation (2%) exhibited less control.

REAFC Model Validation and Implications

The REAFC modeling results presented here support a previous hypothesis explaining high Ni concentrations within the Gamo-Makonnen lavas as the result of high-pressure fractionation of clinopyroxene (George and Rogers, 2002). Specifically, the fractionating assemblage used for our pure fractional crystallization, assimilation, AFC, and REAFC models is dominated by clinopyroxene (modal abundance between 50-60%). Despite the modal abundance of clinopyroxene used, pure fractional crystallization, assimilation, and AFC fail to replicate the Ni concentrations in the Gamo-Makonnen lavas. However, the REAFC solutions result in the observed high Ni concentrations that occur at modest MgO contents, comparable to the Gamo-Makonnen dataset. This effect is the result of Ni becoming buffered in the magmatic system. A similar outcome is observed for Cr where only

REAFC can reproduce the Cr concentrations in the Gamo-Makonnen lavas. The REAFC modeling results confirm that fractionation of clinopyroxene played an important role in the evolution of the Gamo-Makonnen lavas (George and Rogers, 2002), but further refine the mechanism by which magma differentiation proceeded.

The variable buffering of individual elements within the REAFC system can explain the observed differences in incompatible trace element ratios between the Amaro Basalts and the Gamo-Makonnen unit. Previous study of the incompatible trace element and isotopic characteristics of the Amaro and Gamo Basalts indicated it was not possible to generate the Gamo Basalts from the Amaro Basalts through differentiation (George and Rogers, 2002). Our fractional crystallization results support this assertion in that Nb/La values are insufficiently low to capture the Gamo-Makonnen dataset. However, through REAFC, a greater diversity of Nb/La values is possible. The heterogeneity in incompatible trace element ratios between the Amaro Basalts and the Gamo-Makonnen unit can be explained by differential buffering of these elements. Differences in the interval at which a particular incompatible trace element may buffer – e.g., La between 50 and 90 overturns; Nb between 40 and 60 overturns – will result in variance in the ratios of incompatible trace elements.

A final implication of the model results is the potential origin of the Gamo-Makonnen lavas. Our initial rationale for undertaking REAFC modelling was to examine the hypothesis of whether the Gamo-Makonnen lavas could be derived from the Amaro Basalt magmas through differentiation. The primary difference between the Amaro Basalts and the Gamo-Makonnen unit is the incompatible trace element enrichment. Our REAFC model resolves the origin of the observed incompatible trace element enrichment that defines the Gamo-Makonnen magmatic unit as resulting from continued recharge and differentiation within the magma plumbing system (Figure 6). Incompatible trace elements fail to buffer until 20-90 overturns have occurred, while MgO buffers after three overturns. Such modeling outcomes suggest that while MgO and compatible elements may remain constant, the concentration of incompatible trace elements may exhibit substantial variability. The primary outcome of our modelling is that the incompatible trace element concentrations observed in the Gamo-Makonnen lavas can be produced from a parental magma equivalent to the composition of the Amaro Basalt magmas (Figure 6).

Development of the of the Main phase of the Eocene Flood Basalt Magmatic System

Initial Immature Magmatic System

The maturation of a magmatic plumbing system is best probed when a temporal magmatic record exists. The flood basalt component of continental LIPs provide an unusually complete record of magmatic conditions within the lithosphere. The existing stratigraphic constraints show that the earliest manifestations of volcanism within the Eocene continental LIP are represented by the Akobo Basalts (49-46 Ma). These basalts, which exhibit a clear Type II magma signature (Rooney et al., 2017), are derived from the sub-continental lithospheric mantle either through direct melting or foundering of the material into the asthenosphere. The relatively shallow depth of origin of the Akobo Basalts (i.e., within the sub-continental lithospheric mantle) may conflict with the clear evidence of significant fractionation of HREE within the data we present (Tb_{CN}/Yb_{CN} ~2.3). Such fractionation may be considered reflective of deep mantle melting within the garnet zone, if interpreted on the basis of a peridotite melting paradigm. However, fractionated HREE values are commonly seen within melts derived from continental lithosphere metasomes where garnet is inferred to be absent (Rooney, 2020c; Rooney et al., 2017). With a single sample it is difficult to establish the nature of the magmatic

plumbing system during this initial phase, but the limited distribution of this unit is indicative of a poorly developed magmatic plumbing system.

The transition from the initial phase to the main phase of flood basalt volcanism is represented by the Amaro Basalts (45-39 Ma). The initial conditions under which magmatic differentiation occurred during the main phase within the African lithosphere is preserved in the geochemical characteristics of the Amaro Basalts. We propose that the magmatic system active during Amaro Basalt event was dominated by early crystallization of olivine; a secondary, less pronounced, nascent magma system formed at mid-upper crustal levels wherein plagioclase, clinopyroxene, and further olivine fractionates (George and Rogers, 2002). We interpret the diversity in the Amaro Basalt lava compositions as reflecting the relative immaturity of this magmatic system; the lack of an extensive and continuous mid-crustal differentiation system permits melt extraction at various degrees of evolution from a variety of staging chambers throughout the crust (Figure 7).

It is not currently possible to probe the melting conditions within the Akobo Basalt unit due to ambiguities as to the precise modal mineralogy of its lithospheric mantle source. However, existing constraints on magma generation conditions during the subsequent Amaro Basalt phase indicate a relatively high degree of melting to generate the magmas entering the nascent flood basalt plumbing system. The primary Amaro Basalt magmas are hypothesized to be a 6-8% partial melt of a mantle exhibiting elevated mantle potential temperature (~1500 °C) (George and Rogers, 2002; Rooney et al., 2012). This requires a shift in the source of magmatism from the lithosphere to the sub-lithospheric reservoir coincident with the transition from initial to main phase volcanism in the Eocene continental LIP.

Development of a Mature Magmatic System during the Main phase

The eruption of the Gamo-Makonnen magmatic unit (38-28 Ma) is coincident with a profound change in the regional magmatic plumbing system reflective of the maturation of the magma plumbing system during the main phase of flood basalt volcanism. We show that the compositional characteristics of the Gamo-Makonnen lavas can be effectively described by a mature REAFC system within the crust. The efficiency of these magmatic plumbing systems is evident when considering the composition of the erupted products; Gamo-Makonnen lavas are more homogenous than the prior Amaro Basalts and are universally evolved (4.5-6 wt. % MgO), requiring extensive magma hybridization and fractional crystallization. Given the mass removal required during magmatic differentiation within such a system, the flux of magma into the lithosphere during the mature main phase (in comparison to the Amaro Basalt phase) must be far greater than the volume difference in erupted lavas alone. We have shown that the Gamo-Makonnen lavas represent the most volumetrically important unit within the Eocene continental LIP, with the implication that a significantly greater volume of magma moved through the magmatic plumbing system in comparison to the prior Amaro Basalt phase.

The inferred increase of magma volume entering the lithosphere during the Gamo-Makonnen phase has implications for the state of the East African mantle during the main phase of flood basalt volcanism during the Eocene and Oligocene. Increased magma volume during the Gamo-Makonnen event may be achieved through either: (1) a greater degree of melting of the same mantle volume that melted during the Amaro Basalt event, or (2) through melt generation in a larger volume of mantle. The first model is improbable, as a higher degree of melting will result in primitive lavas with even less enrichment in incompatible trace elements than the Amaro Basalts – contrary to observations of enriched lavas from the Gamo-Makonnen unit. The second model may be achieved by decompression melting of the plume material either through thermo-mechanical erosion of the continental lithosphere by the plume itself, or thinning of the continental lithosphere by extension.

George and Rogers (2002) noted that some lithospheric thinning in addition to anomalously hot asthenosphere was required to explain the Palaeogene magmatism. Confirmation of the onset of rifting in this part of Africa is complicated by the superposition of a largely amagmatic Mesozoic rift zone and the magma-rich Cenozoic rift system. Thermal subsidence modelling of the Mesozoic rifting in South Sudan and NW Kenya indicate that a lithospheric thin zone most likely underlay westernmost Ethiopia and the region of the Turkana depression (e.g. Ebinger and Sleep, 1998; Hendrie et al., 1994; Mechie et al., 1994). Basins in the Mesozoic Anza graben east of Lake Turkana showed uplift, erosion, and inversion in a time interval loosely bracketed between 40 and 25 Ma (Morley et al., 1999a). Basins west of Lake Turkana experienced fault-controlled subsidence by roughly 35 Ma, based on paleontological analyses of well data, and stratigraphic ties to surface outcrops (Morley et al., 1999b; Talbot et al., 2004). Fission track data suggest a protracted period of uplift and erosion from ~54 Ma, with clear indications of footwall uplift by ~30 Ma (Boone et al., 2019). The amount of lithospheric stretching in Palaeogene time predicted by subsidence modelling is small (~10%, Emishaw and Abdelsalam, 2019; Hendrie et al., 1994)). The pre-rift lithospheric structure as well as minor stretching within and adjacent to the Mesozoic rift system, therefore, may have served to enhance melting across a much broader region where some minor additional extension occurred (e.g. Ebinger and Sleep, 1998; Hendrie et al., 1994). As outlined above and in Figure 7a, the hydration state of the subcontinental lithospheric mantle (SCLM) may have played a critical role in the localization of the first pulse of magmatism, which occurred within NNW-trending terranes accreted during the Pan-African orogeny (Davidson, 1983). We interpret the increase in magma generation between 38 and 28 Ma as interaction of a deep mantle upwelling with a pre-existing lithospheric thin zone which began to extend, focusing decompression melting of a thermochemically anomalous material to areas with developing magmatic plumbing systems from the initial heating phase. The dikes and sills from the Eocene continental LIP magmatism probably provided warmer, weaker zones for subsequent intrusions, and served to localize the surface expression of magmatism, and may explain the relatively minor crustal contamination of later sequences (George and Rogers, 2002). Thus, the long-lived Gamo-Makonnen sequence with moderate magma production rates exploited the Akobo and Amaro horst plumbing systems, further preconditioning the lithosphere for strain localization as Arabia separated from Africa during the Oligocene. Dynamic processes led to initial extension in the East African rift south of Afar during the early Miocene.

While the transition to a mature plumbing system is coincident with a significant increase in magma volumes, the magmatic system continued to evolve throughout the main phase of Eocene volcanism. The existing dataset shows no clear spatial clustering of Main phase lavas wherein erupted compositions at one locale are best accommodated with a specific input composition. Instead, the variance in samples requires that the three different initial magma types are widely distributed throughout the province. Examination of potential temporal heterogeneity in the magmatic system is more complex and limited by the lack of clear stratigraphic constraints for most samples. Insights into the continued development of the magmatic plumbing system is revealed by the examination of the Bek'ule (1, Figure 1) stratigraphic section, which consists of ~200 m of stratigraphy correlating to 3.5 Ma of time (George and Rogers, 2002). A series of six Gamo Basalt lava samples from this section show lava compositions that become gradually more evolved, decreasing from 6 wt. % MgO in the older flows to ~4 wt. % in the younger flows. These lavas are representative of the entire range of compositions evident within the Gamo-Makonnen dataset. Such an observation suggests some temporal variation in the initial/recharge magma compositions entering the REAFC system, which are becoming more evolved over time, likely reflecting increased residence time (and olivine and clinopyroxene removal) in the deeper part of the magmatic plumbing system. Further refinement of the temporal evolution of the magmatic plumbing system during the main phase requires more complete stratigraphic sampling of lavas from well constrained lava sections.

Connection to the Oligocene Flood Basalt Province

Stratigraphic parallels between the Eocene and Oligocene Provinces

The range of radiogenic age dates (34.8-28.8 Ma) recorded from the Makonnen Basalts of the Gamo-Makonnen magmatic unit show that the eruption of this stratigraphic unit is contemporaneous with the ca. 32–27 Ma Oligocene continental LIP described along the Red Sea margins (Abbate et al., 2014; Baker et al., 1996; Hofmann et al., 1997; Kappelman et al., 2003). On the basis of proximity and these existing geochronological constraints, Rooney (2017) hypothesized that the Makonnen Basalts may have been associated with the Oligocene continental LIP but noted additional geochemical data was needed to confirm this tentative assignation. The new geochemical data we present clearly show that the Makonnen Basalts are magmatically continuous with the Gamo Basalts, forming the Gamo-Makonnen magmatic unit as the predominant composition within the Eocene Province. This conclusion, however, does not preclude a genetic association between the Gamo-Makonnen magmatic unit and the Oligocene continental LIP.

The stratigraphic similarities between the Makonnen Basalts and the Oligocene continental LIP warrant further exploration. The observation of an angular unconformity and paleosol suggests a potential temporal break between the eruption of the Gamo and Makonnen Basalts; these features have been seen elsewhere in the NW Ethiopian Plateau. The initial stratigraphic division of magmatism on the NW Ethiopian plateau recognized that the lower Ashangi was separated from the Aiba flood basalts by an angular unconformity (Mohr and Zanettin, 1988; Zanettin et al., 1980). This observation resulted in the initial division of the Oligocene flood basalts, though this division was ambiguous elsewhere in the province (Mohr, 1983). It is therefore evident that an angular unconformity exists at ca. 30 Ma in both provinces, consistent with evidence of localized extension throughout the region during this period (Bosworth, 1992; Bosworth and Morley, 1994; Hendrie et al., 1994; Purcell, 2018; Tiercelin et al., 2012; Wolfenden et al., 2005).

Geochemical Parallels between the Eocene and Oligocene Provinces

One of the more pronounced features of the Oligocene continental LIP is a distinct spatial zoning of magma types. Stratigraphic units within the flood basalts of the Oligocene continental LIP have been divided on the basis of their magmatic composition. The Ashangi-Aiba stratigraphic units of the Oligocene Province were divided into HT1, HT2, and LT magmatic units (Figure 1) (Beccaluva et al., 2009; Pik et al., 1999, 1998). However, the geometry of the geochemical zonation within the Oligocene continental LIP is complicated due to dissection of the volcanic pile during the opening of the Red Sea and East African Rift (Bellahsen et al., 2003; Wolfenden et al., 2005). Several zonation geometries have been proposed for the Oligocene continental LIP including an E-W bilateral arrangement (Pik et al., 1998) and a "bullseye pattern" of magma types (Furman et al., 2016). On the NW Ethiopian plateau, there is a well-defined bilateral zonation between the LT and HT magma types, where the LT lavas occur only in the west and the HT lavas occur in the east (Pik et al., 1998). Subsequent refinement of the distribution of the HT1 and HT2 lavas resulted in the recognition of a radial component, whereby the HT2 lavas appear to be centered on a volcanic plateau that once linked Ethiopia and Yemen (Beccaluva et al., 2009; Natali et al., 2011). These observations were later reinterpreted by Furman et al. (2016) to represent a bullseye pattern, where the HT2 lavas are centrally located. Examination of flood basalts on the southeastern plateau indicates that volcanism may have initiated somewhat later than the rest of the province and dominantly erupted lavas of an HT affinity (Nelson et al., 2019). These studies thus demonstrate that there is a spatial component to the distribution of magma types in the Oligocene continental LIP , but the geometry of this zonation may differ depending on which magma types are being compared.

Defining a parallel zonation within the Eocene continental LIP has not previously been possible due to a lack of geographically distributed geochemical sampling. Our results suggest there is some ambiguity as to whether the Eocene continental LIP could be considered to be zoned in the same manner. There are three broad magma types within the Eocene continental LIP: the Type II magmas

of the Akobo Basalts and the Balsea Koromto lavas; the depleted-Type Ib of the Amaro Basalts; and the enriched-Type Ib of the Gamo-Makonnen magmatic unit (Rooney, 2017). The Type II lavas in the Eocene continental LIP, which are compositionally equivalent to the HT2 lavas from the Oligocene continental LIP, appear to be volumetrically minor components. The limited volume of Eocene Type II magmas is in stark contrast to the compositionally equivalent HT2 Oligocene lavas, which occupy a large portion of the northern Oligocene continental LIP, extending into Yemen (Beccaluva et al., 2009; Natali et al., 2016; Pik et al., 1999). This dichotomy may relate to the mechanism by which HT2 Oligocene magmas were formed – either through lithosphere foundering (Furman et al., 2016), or in situ melting of the lithospheric mantle (Rooney, 2017; Rooney et al., 2014). Regardless of the potential mechanisms of origin, it is evident that Type II lavas within the Eocene continental LIP do not form a clear spatial domain. If interpreted solely on spatial distribution, it is possible that the more primitive Type Ib Amaro Basalts appear spatially constrained in comparison to the more evolved Type Ib Gamo-Makonnen lavas. However, this spatial zonation is also temporal. Therefore, the Eocene continental LIP does not exhibit the same type of zonation evident within the Oligocene continental LIP.

HT1 lavas from the Oligocene continental LIP compositionally overlap with the Gamo-Makonnen magmatic unit; the HT1 and Gamo-Makonnen lavas exhibit primitive mantle normalised patterns that are broadly sub-parallel (Figure 3). There is a subtle variance between the majority of samples within the Gamo-Makonnen magmatic unit, which exhibit a less fractionated MREE/LREE slope, and the HT1 lavas, which exhibit a more fractionated pattern. This dichotomy is particularly acute when considering the Gamo-Makonnen lava samples from the southern part of the Eocene continental LIP (Main Series/Gamo Basalt stratigraphic unit), which exhibit the least fractionated REE profile. Curiously, as we have noted above, fractionation of REEs within the Gamo-Makonnen magmatic unit increases with proximity to the Oligocene continental LIP (i.e., the Makonnen Basalt stratigraphic unit). A significant barrier in properly comparing the Gamo-Makonnen unit to the HT1 unit is poor sample coverage and the great diversity of lava compositions exhibited by the HT1 lavas. Notably, the broad diversity in compositions evident within the HT1 lava suite is distinct from the relative homogeneity of the Gamo-Makonnen unit. It remains unclear if the HT1 lava samples actually represent the main phase of volcanism within the continental LIP. Therefore, comparison with the Gamo-Makonnen unit may be of limited utility.

The LT lavas of the Oligocene continental LIP exhibit some parallels to the Gamo-Makonnen magmatic unit. Specifically, relative homogeneity of the LT lavas suggests the potential operation of an REAFC system. The LT lavas are classified as Type Ia (Rooney, 2017) and therefore show some broad similarities with the Type Ib magmas of the Gamo-Makonnen unit. However, Type Ia lavas tend to exhibit a greater depletion in most incompatible trace elements with significant anomalies in Ba and Sr in comparison with Type Ib magmas. These observations could tentatively point to similarities in the lavas contributing to the Eocene and Oligocene continental LIP , with some degree of heterogeneity imposed by differing REAFC systems. However, the lack of parallel REAFC modeling on the Oligocene continental LIP prevents more firm conclusions at this time.

Structure of the Magma System and Implications for Rifting of the African Continent

Well-developed magmatic plumbing systems are recognized as being open, transcrustal systems consisting of interconnected intrusions extending from, in some cases, the upper mantle to the upper-most kilometers of the crust (e.g. Cashman et al., 2017). Our work provides new insights into the initiation and evolution of these lithospheric-scale systems, and, indirectly, their role in extensional strain localization. Resolving the crustal levels at which magmas stall are particularly important for understanding how the crust may respond to the large volume of magmas that transit the lithosphere

during LIP events, and those magmas may change the composition of the continental crust. Insight into the distribution of intrusions can be drawn from the mineral modes crystallizing within those intrusions (Morse, 1980). Shallow portions of a continental flood basalt magmatic system, exemplified by the Duluth Complex of Northern Minnesota (Miller and Ripley, 1996; Miller et al. 2002), are dominated by plagioclase crystallization forming troctolites and gabbros (Morse, 1980). However, in the deeper parts of the plumbing system, clinopyroxene is favored (Morse, 1980). The Seiland Igneous Complex in Norway is an example of a lower crustal-upper mantle conduit system that transported tens of thousands of km^3 of magma into the shallower parts of the system (Larsen et al. 2018; Bennet et al., 1986; Grant et al. 2016). Olivine-clinopyroxene cumulates are the predominant rock type in the Seiland Igneous Complex (Larsen et al., 2018) and are inferred to exemplify the deeper portions of the magmatic plumbing system in a continental LIP that transitions to a rift zone. When interpreted within this conceptual framework, the mineral modes required to explain magmatism within the Eocene province are evidence of deep fractionation. Specifically, we have demonstrated that the mass fraction of crystallizing phases required to form the geochemical compositions of lavas within Eocene continental LIP are dominated by clinopyroxene and olivine: 0.22-0.32 ol, 0.5-0.6 cpx, 0.13 plag, and 0.05 oxides. These mass fractions of minerals are consistent with previous studies that interpreted deep-fractionation of clinopyroxene and olivine as strong controls on lava compositions (George and Rogers, 2002). Consequently, we propose that the deep, clinopyroxene-rich component of the magma system feeding the Eocene continental LIP makes up a larger proportion of the fractionating system than the shallower, plagioclase rich component.

Considering the proportions of minerals crystallizing from the REAFC models, and the likely lithologies predicted from the Duluth Complex (shallow) and from the ultramafic component of the Seiland Igneous Complex (deep), we can estimate the volume of material trapped in shallow and deep parts of the magmatic system. Before estimations of the proportion of deep versus shallow intrusion can be performed, the total volume of intruded material needs to be determined. Our REAFC calculations require 2-8% of the total magma be erupted meaning 92-98 % of the total magma remains in the lithosphere as fractionated products. Estimates on the amount of erupted material in the Eocene continental LIP are ~350,000 km^3 (Rooney, 2017). These eruptive volumes translate to a total magma volume ~7 million km^3, of which ~6.65 million km^3 form intrusions throughout the transcrustal magmatic system. If we then assume that the mass fractions of fractionated products calculated by REAFC models presented in this study reflect the approximate depth of emplacement of magmas, it is possible to estimate the volume of intrusive material at left behind at shallow and deep crustal levels as well as in the SCLM.

Crystallization within the Duluth Complex is thought to have occurred between 7.4 and 11.1 km (Miller and Weiblen, 1990) and is dominated by plagioclase-rich assemblages with lesser olivine (dominantly troctolites; Miller et al. 2002). For this reason, we consider the mass fraction of minerals sequestered within the Eocene continental LIP's shallow system to be plagioclase (mass fraction = 0.13) and a portion of olivine (mass fraction = 0.0325), representing a troctolite lithology crystallizing 80% plagioclase and 20% olivine. This translates to an intrusive volume of 1.4 x10^6 km^3 (equivalent to a mass of ~4.8 x 10^{18} kg). The ultramafic intrusions of the Seiland Igneous complex are considered to be the deep crustal roots of Central Iapetus Magmatic Province, intruding between 25-35 km depth, spanning the crust-mantle boundary (Larsen et al. 2018). These deep ultramafic conduits are dominated by clinopyroxene and olivine cumulates (see citations in Larsen et al. 2018). Therefore, we ascribe the crystallizing mass fraction in the deep component of the Eocene continental LIP to dominantly clinopyroxene (mass fraction = 0.6) with the remaining balance assigned to olivine (mass fraction = 0.2875). The deep portion of the magmatic system contains the remaining balance of magma, 5.2 X 10^6 km^3 (equivalent to a mass of ~1.8 x 10^{19} kg). The conclusion that deeper parts of the LIP magmatic system are larger and, therefore, sequester more mass is unsurprising considering

geophysical observations of ~10 km-thick high-velocity underplates beneath Ethiopian plateau and LIPs (Farnetani et al., 1996; Maguire et al., 2006; Thybo and Artemieva, 2013).

The volume of magma released from these deep fractionation systems to shallower crustal levels may be relatively small, but these magmas can have a disproportionate effect on the thermal state of the upper crust. Compared to the relatively hot and dense lower crust, even small volumes of magma intruded in the relatively cool and less dense shallow crust can have a significant impact on crustal rheology (Blundy and Annen, 2016; Schmeling and Wallner, 2012).

Eocene Continental Large Igneous Province and the African LLSVP

The redefined stratigraphy for the Eocene continental LIP requires the main phase of eruption to have taken place over ~10 m.y., far exceeding the <1-3 m.y. main phase of some LIPs. The observation of a 10 m.y.-long main phase is most likely linked to the initiation of extension and lithospheric stretching, and be linked to mantle upwelling beneath cold, stable continental lithosphere. High melt production rates for 2-3 m.y. above a 1000 km-wide plume head is predicted from models (e.g. Campbell and Griffiths, 1990), and observed in some areas (e.g. Jerram and Widdowson, 2005). The rate of melt extraction from the plume head and entrained ambient mantle during the main phase decreases rapidly with time due to either loss of thermal energy or buoyancy to rise and undergo decompression melting (Campbell and Griffiths 1990). In the case of the Deccan and Parana-Etendeka LIPs, each undergo a period of <1-3 m.y characterized by high volcanic flux consistent with rapid melting of the hot mantle plume, yet both are associated with lithospheric thinning during the high magma production phase. The main phase of flood basalt volcanism within the Deccan LIP may have been as short as 750,000 years (Schoene et al., 2019). For the Parana-Etendeka region, significant lithospheric extension occurred during plume head dissipation (e.g., Harry & Sawyer, 1992). The key difference in NE Africa is that little or no lithospheric stretching occurred during the 10 m.y. of slow magma production rates. The highest magma production rates at 32-27 Ma in the Oligocene continental LIP correspond to the onset of crustal extension in what is now the southern Red Sea and Gulf of Aden (Wolfenden et al., 2005), whereas extension in East Africa initiated much later, and exploited the pre-existing crustal magmatic plumbing systems which may have been thermally weakened.

Our results suggest that upwellings from the African LLSVP, often termed the African Superplume (e.g., Ebinger and Sleep, 1998), impinged on cold thick lithosphere which was too strong to extend, or where far-field extension was weak. Instead, melting occurred within pre-existing thin zones of the Mesozoic-Paleaogene Central African rift zone. Lithospheric imaging beneath the area shows a NW–SE-trending high-wavespeed band in southern Ethiopia at <200 km depth, interpreted as refractory Proterozoic lithosphere that has likely influenced the localization of rifting (Kounidis et al., 2021). Only with 10 m.y. of thermal thinning of the lithosphere, and with the development of a widespread system of dikes and sills did lithosphere weaken (e.g., Bialas et al., 2010) to enable rift initiation between 30 and 25 Ma. We present evidence from REAFC models showing that recharge of fresh magma into the magmatic system of the Eocene continental LIP is required to form the erupted lava compositions. The consistency of these lavas compositions through time means that the input of new magma into the system, and by necessity melt generation in the upper mantle, must have been persistent throughout the duration of mafic volcanism. Persistent melting is consistent with elevated mantle potential temperature recorded in lavas in throughout East Africa (Rooney et al., 2012) indicating broad contamination of the upper mantle by warm, upwelling material, potentially derived from the African LLSVP. Contamination of the East African upper mantle by the African LLSVP appears to be widespread, as evidenced by noble gas isotopic characterizations (Haldorssen et al.

2014) and the convergence of radiogenic isotope arrays on a composition broadly equivalent to the Afar Plume (Rooney, 2020c). The broad distribution of high-temperature, LLSVP derived material is consistent with geophysical observations of a broad thermochemical anomaly present within the East African upper mantle (e.g. Bastow et al., 2008; Boyce et al., 2021; Chang et al., 2020). The modern, widespread thermochemical anomaly may have first interacted with the African lithosphere during the Eocene, providing a means to generate the magma supply required to maintain the long-lived magmatic system that formed the Eocene continental LIP in East Africa.

Conclusions

The Eocene continental LIP of SW Ethiopia and northern Kenya is the earliest volcanic manifestation of the interaction between a rising mantle thermochemical anomaly associated with the African LLSVP and the East African lithosphere. The dataset presented herein represents the most geographically distributed suite of lava samples from the Eocene continental LIP, and thus presents an opportunity to resolve an outstanding question of whether geochemical zonation exists within this province that is similar to that observed within the later Oligocene continental LIP . We find that the geochemical variability across the Eocene continental LIP is rather limited – most of the erupted lavas exhibit a trace element pattern that is broadly consistent with the previously characterized Gamo Basalts. An important exception to this homogenous distribution are the Amaro Basalts, which occur in a small area in the east of the province but predate the main phase represented by the Gamo Basalts. The existing data thus show that the Eocene continental LIP lacks the strong geochemical zonation found in the Oligocene continental LIP.

We have shown that lavas of the Eocene continental LIP can be united under a single volcano-stratigraphic framework that records the magmatic evolution of the province. The Cenozoic volcano-stratigraphic record in SW Ethiopia begins at ~49 Ma with the small-volume eruption of the alkaline Akobo Basalts, which we interpret as the result of melting of destabilized mantle metasomes derived from continental lithosphere (Beccaluva et al., 2009; Rooney, 2020c; Rooney et al., 2017, 2014). The occurrence of early-alkaline volcanism is observed in other LIPs (e.g. Parana-Entendeka, Jerram and Widdowson, 2005) including the neighboring province on the NW Ethiopian plateau but is eventually overwhelmed by more voluminous magmas associated with flood basalt eruptions (Jerram et al., 1999, 2000). Prior geochronologic studies have shown that subsequent flood basalt-style volcanism begins with the eruption of the Amaro Basalt (~45-39 Ma), which we suggest is derived from a relatively immature magmatic plumbing system. Subsequent widespread magmatism (~38-28 Ma) is the amalgamation of several stratigraphic units: the Gamo Basalts, the Main Series, and the Makonnen Basalts. We have shown that the major and trace element characteristics of all three stratigraphic units show limited variability and are thus geochemically indistinguishable. Consequently, we combine the Gamo Basalts, the Main Series, and the Makonnen Basalts into a single magmatic unit termed the Gamo-Makonnen magmatic unit.

With an increasing awareness that lavas erupted during main phase volcanism within a LIP may be impacted by complex differentiation (Bohrson et al., 2020, 2014; Lee et al., 2014; Yu et al., 2015) processes, we undertook REAFC magma modelling to constrain the origin of the Gamo-Makonnen magmatic unit. We find that the erupted compositional range of the Gamo-Makonnen Magmatic unit can be produced via REAFC processes. Critically, our modelling shows that the Gamo-Makonnen lavas may be produced from starting compositions equivalent to Amaro Basalt lavas. The implication of these results is the potential continuity of primitive magma compositions supplying the magma differentiation system during the main phase of volcanism for the Eocene continental LIP. The continuity of magma supply during the eruption of the Gamo-Makonnen magmatic unit indicates prolonged melting of mantle-derived material, exceeding the main phase eruptive cycle for a typical continental LIP. Such an observation provides valuable insight into the character of the East African upper mantle.

Cenozoic flood basalts in East Africa provide an unusual opportunity to probe material rising from one of the largest structures on the planet – the African LLSVP (Rooney, 2017). Prolonged magma supply feeding the Gamo-Makonnen magmatic unit combined with the subsequent eruption of the neighboring Oligocene continental LIP is suggestive an upper mantle that is being influenced by thermo-chemically anomalous material over broad spatial and temporal scales. It is possible that material rising from the African LLSVP has contaminated much of East African upper mantle, a hypothesis supported by the widespread isotopic signatures of plume-like material and elevated mantle potential temperatures throughout the region (Rooney, 2020c). The eruption of the Eocene continental LIP marks start of a relationship between the African lithosphere and material derived from the deep mantle that will impact the geologic history of East Africa through modern times. Magmas generated as a result of the interaction of material derived from the African LLSVP and the African lithosphere during the Palaeogene had a profound impact on the thermal and compositional state of the East African crust, contributing to the rupture of the African continent and the formation of the East African Rift system. The intrusion of magmas that would erupt to form Akobo and Amaro basalts created preferred conduits for subsequent main phase lavas of the Gamo-Makonnen magmatic unit. The relative homogeneity of the Gamo-Makonnen lavas is evidence for a magmatic system that underwent magma recharge and mixing, processes that require magma injections into existing magma bodies. Critically, the 10 m.y. long period of magma injection during this phase was required to create the zones of weakness in the African lithosphere and SCLM that would focus strain during Oligo-Miocene extension. These zones of weakness may have been an important component in focusing strain, facilitating the initiation of the East African Rift system.

References

Abbate, E., Bruni, P., Ferretti, M.P., Delmer, C., Laurenzi, M.A., Hagos, M., Bedri, O., Rook, L., Sagri, M., Libsekal, Y., 2014. The East Africa Oligocene intertrappean beds: Regional distribution, depositional environments and Afro/Arabian mammal dispersals. Journal of African Earth Sciences 99, 463–489. https://doi.org/10.1016/j.jafrearsci.2013.11.001

Armitage, J.J., Ferguson, D.J., Goes, S., Hammond, J.O., Calais, E., Rychert, C.A., Harmon, N., 2015. Upper mantle temperature and the onset of extension and break-up in Afar, Africa. Earth Planet Sc Lett 418, 78–90.

Baker, B.H., Williams, L.A.J., Miller, J.A., Fitch, F.J., 1971. Sequence and geochronology of the Kenya rift volcanics. Tectonophysics 11, 191–215. https://doi.org/10.1016/0040-1951(71)90030-8

Baker, J., Snee, L., Menzies, M., 1996. A brief Oligocene period of flood volcanism in Yemen: implications for the duration and rate of continental flood volcanism at the Afro-Arabian triple junction. Earth and Planetary Science Letters 138, 39–55. https://doi.org/10.1016/0012-821X(95)00229-6

Bastow, I., Nyblade, A., Stuart, G., Rooney, T., Benoit, M., 2008. Upper mantle seismic structure beneath the Ethiopian hot spot: Rifting at the edge of the African low-velocity anomaly. Geochemistry, Geophysics, Geosystems 9.

Beccaluva, L., Bianchini, G., Natali, C., Siena, F., 2009. Continental flood basalts and mantle plumes: a case study of the Northern Ethiopian Plateau. J Petrol 50, 1377–1403.

Bellahsen, N., Faccenna, C., Funiciello, F., Daniel, J.M., Jolivet, L., 2003. Why did Arabia separate from Africa? Insights from 3-D laboratory experiments. Earth and Planetary Science Letters 216, 365–381. https://doi.org/10.1016/S0012-821X(03)00516-8

Bellieni, G., Brotzu, P., Morbidelli, L., Piccirillo, E.M., Traversa, G., 1986. Petrology and Mineralogy of Miocene Fissural Volcanism of the East Kenya Plateau. Neues Jb Miner Abh 154, 153–178.

Bennett, M., Emblin, S., Robins, B., Yeo, W., 1986. High-temperature ultramafic complexes in the North-Norwegian Caledonides. I: Regional setting and field relationships. Bulletin-Norges geologiske undersokelse 1–40.

Blundy, J.D., Annen, C.J., 2016. Crustal magmatic systems from the perspective of heat transfer. Elements 12, 115–120.

Bohrson, W.A., Spera, F.J., 2001. Energy-constrained open-system magmatic processes II: Application of energy-constrained assimilation-fractional crystallization (EC-AFC) model to magmatic systems. J Petrol 42, 1019–1041.

Bohrson, W.A., Spera, F.J., Ghiorso, M.S., Brown, G.A., Creamer, J.B., Mayfield, A., 2014. Thermodynamic Model for Energy-Constrained Open-System Evolution of Crustal Magma Bodies Undergoing Simultaneous Recharge, Assimilation and Crystallization: the Magma Chamber Simulator. Journal of Petrology 55, 1685–1717. https://doi.org/10.1093/petrology/egu036

Bohrson, W.A., Spera, F.J., Ghiorso, M.S., Fowler, S.J., 2006. The Magma Chamber Simulator: A comprehensive tool for modeling the evolution of magmatic systems. AGUFM 2006, V11A-0566.

Bohrson, W.A., Spera, F.J., Heinonen, J.S., Brown, G.A., Scruggs, M.A., Adams, J.V., Takach, M.K., Zeff, G., Suikkanen, E., 2020. Diagnosing open-system magmatic processes using the Magma Chamber Simulator (MCS): part I—major elements and phase equilibria. Contributions to Mineralogy and Petrology 175, 1–29.

Boone, S.C., Kohn, B.P., Gleadow, A.J., Morley, C.K., Seiler, C., Foster, D.A., 2019. Birth of the East African Rift System: Nucleation of magmatism and strain in the Turkana Depression. Geology 47, 886–890.

Bosworth, W., 1992. Mesozoic and early Tertiary rift tectonics in East Africa. Tectonophysics 209, 115–137. https://doi.org/10.1016/0040-1951(92)90014-W

Bosworth, W., Morley, C.K., 1994. Structural and stratigraphic evolution of the Anza rift, Kenya. Tectonophysics 236, 93–115.

Bougault, H., Hekinian, R., 1974. Rift Valley in the Atlantic Ocean near 36°50′N: petrology and geochemistry of basaltic rocks. Earth and Planetary Science Letters 24, 249–261. https://doi.org/10.1016/0012-821X(74)90103-4

Boyce, A., Bastow, I.D., Cottaar, S., Kounoudis, R., Guilloud De Courbeville, J., Caunt, E., Desai, S., 2021. AFRP20: New P-Wavespeed Model for the African Mantle Reveals Two Whole-Mantle Plumes Below East Africa and Neoproterozoic Modification of the Tanzania Craton. Geochemistry, Geophysics, Geosystems 22, e2020GC009302.

Boynton, W.V., 1984. Cosmochemistry of the Rare Earth Elements: Meteorite Studies, in: Developments in Geochemistry. Elsevier, pp. 63–114. https://doi.org/10.1016/B978-0-444-42148-7.50008-3

Brotzu, P., Morbidelli, L., Nicoletti, M., Piccirillo, E.M., Traversa, G., 1984. Miocene to quaternary volcanism in eastern Kenya: Sequence and geochronology. Tectonophysics 101, 75–86. https://doi.org/10.1016/0040-1951(84)90043-X

Brown, F.H., McDougall, I., 2011. Geochronology of the Turkana Depression of Northern Kenya and Southern Ethiopia. Evolutionary Anthropology: Issues, News, and Reviews 20, 217–227. https://doi.org/10.1002/evan.20318

Campbell, I.H., Griffiths, R.W., 1990. Implications of mantle plume structure for the evolution of flood basalts. Earth Planet Sc Lett 99, 79–93.

Cashman, K.V., Sparks, R.S.J., Blundy, J.D., 2017. Vertically extensive and unstable magmatic systems: A unified view of igneous processes. Science 355, eaag3055. https://doi.org/10.1126/science.aag3055

Chambers, E.L., Harmon, N., Keir, D., Rychert, C.A., 2019. Using ambient noise to image the northern East African Rift. Geochemistry, Geophysics, Geosystems 20, 2091–2109.

Chang, S.-J., Kendall, E., Davaille, A., Ferreira, A.M., 2020. The evolution of mantle plumes in East Africa. Journal of Geophysical Research: Solid Earth 125, e2020JB019929.

Charlier, B., Namur, O., Latypov, R., Tegner, C. (Eds.), 2015. Layered Intrusions, Springer Geology. Springer Netherlands, Dordrecht. https://doi.org/10.1007/978-94-017-9652-1

Corti, G., Cioni, R., Franceschini, Z., Sani, F., Scaillet, S., Molin, P., Isola, I., Mazzarini, F., Brune, S., Keir, D., Erbello, A., Muluneh, A., Illsley-Kemp, F., Glerum, A., 2019. Aborted propagation of the Ethiopian rift caused by linkage with the Kenyan rift. Nat Commun 10, 1309. https://doi.org/10.1038/s41467-019-09335-2

Cox, K.G., 1980. A Model for Flood Basalt Vulcanism. Journal of Petrology 21, 629–650. https://doi.org/10.1093/petrology/21.4.629

Davidson, A., Moore, J., Davies, J., Alemu Shiferaw, M.T., 1973. Preliminary report on the geology and geochemistry of parts of Sidamo, Gemu Gofa, and Kefa Provinces. Rept. Omo River Project 1.

Davidson, A., Rex, D.C., 1980. Age of volcanism and rifting in southwestern Ethiopia. Nature 283, 657–658. https://doi.org/10.1038/283657a0

Davidson, A.C., 1983. The Omo RIver Project, Reconaissance geology and geochemistry of parts of Ilubabor, Kefa, Gemi Gofa, and Sidamo. Ministry of Mines and Energy: Ethiopian Institute of Geological Surveys Bulletin 2, 1–89.

Ding, X., Ripley, E.M., Li, C., 2012. PGE geochemistry of the Eagle Ni–Cu–(PGE) deposit, Upper Michigan: constraints on ore genesis in a dynamic magma conduit. Mineralium Deposita 47, 89–104. https://doi.org/10.1007/s00126-011-0350-y

Ebinger, C.J., 2020. Recipe for Rifting: Flavors of East Africa.

Ebinger, C.J., Keir, D., Bastow, I.D., Whaler, K., Hammond, J.O., Ayele, A., Miller, M.S., Tiberi, C., Hautot, S., 2017. Crustal structure of active deformation zones in Africa: Implications for global crustal processes. Tectonics 36, 3298–3332.

Ebinger, C.J., Sleep, N.H., 1998. Cenozoic magmatism throughout east Africa resulting from impact of a single plume. Nature 395, 788–791. https://doi.org/10.1038/27417

Ebinger, C.J., Yemane, T., Kelley, S., Rex, D.C., 2000. Rift deflection, migration, and propagation: Linkage of the Ethiopian and Eastern rifts, Africa. Geological Society of America Bulletin 14.

Ebinger, C.J., Yemane, T., Woldegabriel, G., Aronson, J.L., Walter, R.C., 1993. Late Eocene–Recent volcanism and faulting in the southern main Ethiopian rift. Journal of the Geological Society 150, 99–108. https://doi.org/10.1144/gsjgs.150.1.0099

Emishaw, L., Abdelsalam, M.G., 2019. Development of Late Jurassic-Early Paleogene and Neogene-Quaternary Rifts Within the Turkana Depression, East Africa From Satellite Gravity Data. Tectonics 38, 2358–2377.

Ernst, R.E., 2014. Large Igneous Provinces. Cambridge University Press, Cambridge, United Kingdom.

Ewart, A., Griffin, W.L., 1994. Application of proton-microprobe data to trace-element partitioning in volcanic rocks. Chemical Geology 117, 251–284.

Faccenna, C., Glišović, P., Forte, A., Becker, T.W., Garzanti, E., Sembroni, A., Gvirtzman, Z., 2019. Role of dynamic topography in sustaining the Nile River over 30 million years. Nat. Geosci 12, 1012–1017.

Farnetani, C.G., Richards, M.A., Ghiorso, M.S., 1996. Petrological models of magma evolution and deep crustal structure beneath hotspots and flood basalt provinces. Earth Planet Sc Lett 143, 81–94.

Ferguson, D.J., Maclennan, J., Bastow, I.D., Pyle, D.M., Jones, S.M., Keir, D., Blundy, J.D., Plank, T., Yirgu, G., 2013. Melting during late-stage rifting in Afar is hot and deep. Nature 499, 70–73. https://doi.org/10.1038/nature12292 http://www.nature.com/nature/journal/v499/n7456/abs/nature12292.html#supplementary-information

Furman, T., Kaleta, K.M., Bryce, J.G., Hanan, B.B., 2006. Tertiary Mafic Lavas of Turkana, Kenya: Constraints on East African Plume Structure and the Occurrence of High-µ Volcanism in Africa. Journal of Petrology 47, 1221–1244. https://doi.org/10.1093/petrology/egl009

Furman, T., Nelson, W.R., Elkins-Tanton, L.T., 2016. Evolution of the East African rift: Drip magmatism, lithospheric thinning and mafic volcanism. Geochimica et Cosmochimica Acta 185, 418–434. https://doi.org/10.1016/j.gca.2016.03.024

George, R., Rogers, N., 2002. Plume dynamics beneath the African plate inferred from the geochemistry of the Tertiary basalts of southern Ethiopia. Contributions to Mineralogy and Petrology 144, 286–304. https://doi.org/10.1007/s00410-002-0396-z

George, R., Rogers, N., Kelley, S., 1998. Earliest magmatism in Ethiopia: Evidence for two mantle plumes in one flood basalt province. Geology 26, 923. https://doi.org/10.1130/0091-7613(1998)026<0923:EMIEEF>2.3.CO;2

Grant, T.B., Larsen, R.B., Anker-Rasch, L., Grannes, K.R., Iljina, M., McEnroe, S., Nikolaisen, E., Schanche, M., Øen, E., 2016. Anatomy of a deep crustal volcanic conduit system; the Reinfjord ultramafic complex, Seiland Igneous Province, northern Norway. Lithos 252, 200–215.

Green, T.H., Blundy, J.D., Adam, J., Yaxley, G.M., 2000. SIMS determination of trace element partition coefficients between garnet, clinopyroxene and hydrous basaltic liquids at 2–7.5 GPa and 1080–1200 C. Lithos 53, 165–187.

Griselin, M., Arndt, N.T., Baragar, W.R.A., 1997. Plume–lithosphere interaction and crustal contamination during formation of Coppermine River basalts, Northwest Territories, Canada. Can. J. Earth Sci. 34, 958–975. https://doi.org/10.1139/e17-080

Guth, A.L., 2013. Spatial and Temporal Evolution of the Volcanics and Sediments of the Kenya Rift. Michigan Technological University.

Hackman, B.D., Charsley, T.J., Key, R.M., Wilkinson, A.F., 1990. The development of the East African Rift system in north-central Kenya. Tectonophysics 184, 189–211. https://doi.org/10.1016/0040-1951(90)90053-B

Hendrie, D.B., Kusznir, N.J., Morley, C.K., Ebinger, C.J., 1994. Cenozoic extension in Northern Kenya - A quantitative model of rift basin development in the Turkana region. Tectonophysics 236, 409–438.

Hofmann, C., Courtillot, V., Féraud, G., Rochette, P., Yirgu, G., Ketefo, E., Pik, R., 1997. Timing of the Ethiopian flood basalt event and implications for plume birth and global change. Nature 389, 838–841. https://doi.org/10.1038/39853

Jean, M.M., Shervais, J.W., Champion, D.E., Vetter, S.K., 2013. Geochemical and paleomagnetic variations in basalts from the Wendell Regional Aquifer Systems Analysis (RASA) drill core: Evidence for magma recharge and assimilation–fractional crystallization from the central Snake River Plain, Idaho. Geosphere 9, 1319. https://doi.org/10.1130/GES00914.1

Jerram, D., Mountney, N., Holzförster, F., Stollhofen, H., 1999. Internal stratigraphic relationships in the Etendeka group in the Huab Basin, NW Namibia: understanding the onset of flood volcanism. Journal of Geodynamics 28, 393–418. https://doi.org/10.1016/S0264-3707(99)00018-6

Jerram, D.A., Mountney, N.P., Howell, J.A., Long, D., Stollhoffen, H., 2000. Death of a sand sea: an active aeolian erg systematically buried by the Etendeka flood basalts of NW Namibia. Journal of the Geological Society 157, 513. https://doi.org/10.1144/jgs.157.3.513

Jerram, D.A., Widdowson, M., 2005. The anatomy of Continental Flood Basalt Provinces: geological constraints on the processes and products of flood volcanism. Lithos 79, 385–405. https://doi.org/10.1016/j.lithos.2004.09.009

Kappelman, J., Tab Rasmussen, D., Sanders, W.J., Feseha, M., Bown, T., Copeland, P., Crabaugh, J., Fleagle, J., Glantz, M., Gordon, A., Jacobs, B., Maga, M., Muldoon, K., Pan, A., Pyne, L., Richmond, B., Ryan, T., Seiffert, E.R., Sen, S., Todd, L., Wiemann, M.C., Winkler, A., 2003. Oligocene mammals from Ethiopia and faunal exchange between Afro-Arabia and Eurasia. Nature 426, 549–552. http://www.nature.com/nature/journal/v426/n6966/suppinfo/nature02102_S1.html

Key, R.M., Watkins, R.T., 1988. Geology of the Sabarei area. Republic of Kenya Ministry of Environment and Natural Resources, Mines and Geological Department Report 111.

Kieffer, B., Arndt, N., Lapierre, H., Bastien, F., Bosch, D., Pecher, A., Yirgu, G., Ayalew, D., Weis, D., Jerram, D.A., Keller, F., Meugniot, C., 2004. Flood and Shield Basalts from Ethiopia: Magmas from the African Superswell. Journal of Petrology 45, 793–834. https://doi.org/10.1093/petrology/egg112

Kounoudis, R., Bastow, I.D., Ebinger, C.J., Ogden, C.S., Ayele, A., Bendick, R., Mariita, N., Kianji, G., Wigham, G., Musila, M., Kibret, B., 2021. Body-wave tomographic imaging of the Turkana Depression: Implications for rift development and plume-lithosphere interactions. Geochem Geophys Geosyst. https://doi.org/10.1029/2021GC009782

Krans, S.R., Rooney, T.O., Kappelman, J., Yirgu, G., Ayalew, D., 2018. From initiation to termination: a petrostratigraphic tour of the Ethiopian Low-Ti Flood Basalt Province. Contributions to Mineralogy and Petrology 173. https://doi.org/10.1007/s00410-018-1460-7

Larsen, R.B., Grant, T., Sørensen, B.E., Tegner, C., McEnroe, S., Pastore, Z., Fichler, C., Nikolaisen, E., Grannes, K.R., Church, N., ter Maat, G.W., Michels, A., 2018. Portrait of a giant deep-seated magmatic conduit system: The Seiland Igneous Province. Lithos 296–299, 600–622. https://doi.org/10.1016/j.lithos.2017.11.013

Lassiter, J.C., DePAOLO, D.J., Mahoney, J.J., 1995. Geochemistry of the Wrangellia Flood Basalt Province: Implications for the Role of Continental and Oceanic Lithosphere in Flood Basalt Genesis. Journal of Petrology 36, 983–1009. https://doi.org/10.1093/petrology/36.4.983

Lavayssière, A., Rychert, C., Harmon, N., Keir, D., Hammond, J.O., Kendall, J.-M., Doubre, C., Leroy, S., 2018. Imaging lithospheric discontinuities beneath the Northern East African Rift using S-to-P receiver functions. Geochemistry, Geophysics, Geosystems 19, 4048–4062.

Lee, C.-T.A., Lee, T.C., Wu, C.-T., 2014. Modeling the compositional evolution of recharging, evacuating, and fractionating (REFC) magma chambers: Implications for differentiation of arc magmas. Geochimica et Cosmochimica Acta 143, 8–22. https://doi.org/10.1016/j.gca.2013.08.009

Lightfoot, P.C., Naldrett, A.J., Gorbachev, N.S., Doherty, W., Fedorenko, V.A., 1990. Geochemistry of the Siberian Trap of the Noril'sk area, USSR, with implications for the relative contributions of crust and mantle to flood basalt magmatism. Contr. Mineral. and Petrol. 104, 631–644. https://doi.org/10.1007/BF01167284

Maguire, P.K.H., Keller, G.R., Klemperer, S.L., Mackenzie, G.D., Keranen, K., Harder, S., O'Reilly, B., Thybo, H., Asfaw, L., Khan, M.A., Amha, M., 2006. Crustal structure of the northern Main Ethiopian Rift from the EAGLE controlled-source survey; a snapshot of incipient lithospheric break-up. Geological Society, London, Special Publications 259, 269–292. https://doi.org/10.1144/GSL.SP.2006.259.01.21

Maitre, L., 1989. A classification of igneous rocks and glossary of terms. Recommendations of the international union of geological sciences subcommission on the systematics of igneous rocks 193.

McCallum, I.S., Charette, M.P., 1978. Zr and Nb partition coefficients: Implications for the genesis of mare basalts, KREEP and sea floor basalts. Geochimica et Cosmochimica Acta 42, 859–869. https://doi.org/10.1016/0016-7037(78)90098-4

McDougall, I., Watkins, R.T., 2006. Geochronology of the Nabwal Hills: a record of earliest magmatism in the northern Kenyan Rift Valley. Geological Magazine 143, 25–39. https://doi.org/10.1017/S0016756805001184

McKenzie, D., O'Nions, R.K., 1991. Partial Melt Distributions from Inversion of Rare-Earth Element Concentrations. J Petrol 32, 1021–1091.

Mechie, J., Keller, G.R., Prodehl, C., Gaciri, S., Braile, L.W., Mooney, W.D., Gajewski, D., Sandmeier, K.-J., 1994. Crustal structure beneath the Kenya Rift from axial profile data. Tectonophysics 236, 179–200.

Mohr, P., 1983. Ethiopian flood basalt province. Nature 303, 577–584.

Mohr, P., Zanettin, B., 1988. The Ethiopian flood basalt province, in: MacDougall, J.D. (Ed.), Continental Flood Basalts. Kluwer Academic, Dordrecht, pp. 63–110.

Montési, L.G., 2013. Fabric development as the key for forming ductile shear zones and enabling plate tectonics. Journal of Structural Geology 50, 254–266.

Morley, C.K., Bosworth, W., Day, R.A., Lauck, R., Bosher, R., Stone, D.M., Wigger, S.T., Wescott, W.A., Haun, D., Bassett, N., 1999a. AAPG Studies in Geology# 44, Chapter 4: Geology and Geophysics of the Anza Graben.

Morley, C.K., Karanja, F.M., Wescott, W.A., Stone, D.M., Harper, R.M., Wigger, S.T., Day, R.A., 1999b. AAPG Studies in Geology# 44, Chapter 2: Geology and Geophysics of the Western Turkana Basins, Kenya.

Morley, C.K., Wescott, W.A., Stone, D.M., Harper, R.M., Wigger, S.T., Karanja, F.M., 1992. Tectonic evolution of the Northern Kenyan rift. Journal of the Geological Society 149, 333–348.

Naldrett, A.J., 2010. Secular Variation of Magmatic Sulfide Deposits and Their Source Magmas. Economic Geology 105, 669–688. https://doi.org/10.2113/gsecongeo.105.3.669

Natali, C., Beccaluva, L., Bianchini, G., Ellam, R.M., Savo, A., Siena, F., Stuart, F.M., 2016. High-MgO lavas associated to CFB as indicators of plume-related thermochemical effects: The case of ultra-titaniferous picrite–basalt from the Northern Ethiopian–Yemeni Plateau. Gondwana Research 34, 29–48.

Natali, C., Beccaluva, L., Bianchini, G., Siena, F., 2013. The Axum–Adwa basalt–trachyte complex: a late magmatic activity at the periphery of the Afar plume. Contrib Mineral Petr 166, 351–370. https://doi.org/10.1007/s00410-013-0879-0

Natali, C., Beccaluva, L., Bianchini, G., Siena, F., 2011. Rhyolites associated to Ethiopian CFB: clues for initial rifting at the Afar plume axis. Earth Planet Sc Lett 312, 59–68.

Nelson, W.R., Hanan, B., Graham, D.W., Shirey, S.B., Yirgu, G., Ayalew, D., Furman, T., 2019. Distinguishing plume and metasomatized lithospheric mantle contributions to post-flood basalt volcanism on the southeastern Ethiopian Plateau. Journal of Petrology.

Nielsen, R.L., Gallahan, W.E., Newberger, F., 1992. Experimentally determined mineral-melt partition coefficients for Sc, Y and REE for olivine, orthopyroxene, pigeonite, magnetite and ilmenite. Contributions to Mineralogy and Petrology 110, 488–499.

Nishimura, K., 2019. Chemical mass balance equations for open-system magma chamber processes that result in crystal zoning. Journal of Volcanology and Geothermal Research 374, 181–196. https://doi.org/10.1016/j.jvolgeores.2019.02.012

Paces, J.B., 1990. Magmatic processes, evolution and mantle source characteristics contributing to the petrogenesis of midcontinent rift basalts: Portage Lake volcanics, Keweenaw Peninsula, Michigan.

Paster, T.P., Schauwecker, D.S., Haskin, L.A., 1974. The behavior of some trace elements during solidification of the Skaergaard layered series. Geochimica et Cosmochimica Acta 38, 1549–1577. https://doi.org/10.1016/0016-7037(74)90174-4

Peng, Z.X., Mahoney, J., Hooper, P., Harris, C., Beane, J., 1994. A role for lower continental crust in flood basalt genesis? Isotopic and incompatible element study of the lower six formations of the western Deccan Traps. Geochimica et Cosmochimica Acta 58, 267–288. https://doi.org/10.1016/0016-7037(94)90464-2

Pik, R., Deniel, C., Coulon, C., Yirgu, G., Hofmann, C., Ayalew, D., 1998. The northwestern Ethiopian Plateau flood basalts: Classification and spatial distribution of magma types. Journal of Volcanology and Geothermal Research 81, 91–111. https://doi.org/10.1016/S0377-0273(97)00073-5

Pik, R., Deniel, C., Coulon, C., Yirgu, G., Marty, B., 1999. Isotopic and trace element signatures of Ethiopian flood basalts; evidence for plume-lithosphere interactions. Geochim Cosmochim Ac 63, 2263–2279.

Pik, R., Marty, B., Carignan, J., Yirgu, G., Ayalew, T., 2008. Timing of East African Rift development in southern Ethiopia: Implication for mantle plume activity and evolution of topography. Geology 36, 167–170.

Priestley, K., McKenzie, D., Debayle, E., Pilidou, S., 2008. The African upper mantle and its relationship to tectonics and surface geology. Geophys J Int 175, 1108–1126.

Purcell, P.G., 2018. Re-imagining and re-imaging the development of the East African Rift. Petroleum Geoscience 24, 21–40. https://doi.org/10.1144/petgeo2017-036

Reed, C.A., Gao, S.S., Liu, K.H., Yu, Y., 2016. The mantle transition zone beneath the Afar Depression and adjacent regions: Implications for mantle plumes and hydration. Geophysical Journal International 205, 1756–1766.

Ridley, V.A., Richards, M.A., 2010. Deep crustal structure beneath large igneous provinces and the petrologic evolution of flood basalts. Geochemistry, Geophysics, Geosystems 11. https://doi.org/10.1029/2009GC002935

Ringwood, A.E., Essene, E., 1970. Petrogenesis of Apollo 11 basalts, internal constitution and origin of the moon. Geochimica et Cosmochimica Acta Supplement 1, 769.

Rochette, P., Tamrat, E., Féraud, G., Pik, R., Courtillot, V., Ketefo, E., Coulon, C., Hoffmann, C., Vandamme, D., Yirgu, G., 1998. Magnetostratigraphy and timing of the Oligocene Ethiopian traps. Earth and Planetary Science Letters 164, 497–510. https://doi.org/10.1016/S0012-821X(98)00241-6

Rogers, N.W., Thomas, L.E., Macdonald, R., Hawkesworth, C.J., Mokadem, F., 2006. U-238-Th-230 disequilibrium in recent basalts and dynamic melting beneath the Kenya rift. Chem Geol 234, 148–168. https://doi.org/DOI 10.1016/j.chemgeo.2006.05.002

Rooney, T., Franceschi, P., Hall, C., 2011. Water-saturated magmas in the Panama Canal region: a precursor to adakite-like magma generation? Contrib Mineral Petr 161, 373–388. https://doi.org/10.1007/s00410-010-0537-8

Rooney, T.O., 2020a. The Cenozoic magmatism of East Africa: Part II – Rifting of the mobile belt. Lithos 360–361, 105291. https://doi.org/10.1016/j.lithos.2019.105291

Rooney, T.O., 2020b. The Cenozoic magmatism of East Africa: Part III – Rifting of the craton. Lithos 105390. https://doi.org/10.1016/j.lithos.2020.105390

Rooney, T.O., 2020c. The Cenozoic magmatism of East Africa: part V–magma sources and processes in the East African Rift. Lithos 360, 105296.

Rooney, T.O., 2017. The Cenozoic magmatism of East-Africa: Part I — Flood basalts and pulsed magmatism. Lithos 286–287, 264–301. https://doi.org/10.1016/j.lithos.2017.05.014

Rooney, T.O., 2010. Geochemical evidence of lithospheric thinning in the southern Main Ethiopian Rift. Lithos 117, 33–48. https://doi.org/10.1016/j.lithos.2010.02.002

Rooney, T.O., Herzberg, C., Bastow, I.D., 2012. Elevated mantle temperature beneath East Africa. Geology 40, 27–30. https://doi.org/10.1130/G32382.1

Rooney, T.O., Morell, K.D., Hidalgo, P., Fraceschi, P., 2015. Magmatic consequences of the transition from orthogonal to oblique subduction in P anama. Geochemistry, Geophysics, Geosystems 16, 4178–4208. https://doi.org/10.1002/2015GC006150

Rooney, T.O., Nelson, W.R., Ayalew, D., Hanan, B., Yirgu, G., Kappelman, J., 2017. Melting the lithosphere: Metasomes as a source for mantle-derived magmas. Earth and Planetary Science Letters 461, 105–118. https://doi.org/10.1016/j.epsl.2016.12.010

Rooney, T.O., Nelson, W.R., Dosso, L., Furman, T., Hanan, B., 2014. The role of continental lithosphere metasomes in the production of HIMU-like magmatism on the northeast African and Arabian plates. Geology 42, 419–422. https://doi.org/10.1130/G35216.1

Rudnick, R., Gao, S., 2003. Composition of the continental crust, in: Rudnick, R. (Ed.), The Crust, Treatise on Geochemistry. Elsevier-Pergamon, Oxford, pp. 1–64.

Schmeling, H., Wallner, H., 2012. Magmatic lithospheric heating and weakening during continental rifting: A simple scaling law, a 2-D thermomechanical rifting model and the East African Rift System. Geochemistry, Geophysics, Geosystems 13.

Schoene, B., Eddy, M.P., Samperton, K.M., Keller, C.B., Keller, G., Adatte, T., Khadri, S.F., 2019. U-Pb constraints on pulsed eruption of the Deccan Traps across the end-Cretaceous mass extinction. Science 363, 862–866.

Self, S., Thordarson, T., Keszthelyi, L., 1997. Emplacement of continental flood basalt lava flows. Geophysical Monograph-AGU 100, 381–410.

Self, S., Thordarson, T., Widdowson, M., 2005. Gas fluxes from flood basalt eruptions. Elements 1, 283–287.

Spera, F.J., Bohrson, W.A., 2001. Energy-constrained open-system magmatic processes I: General model and energy-constrained assimilation and fractional crystallization (EC-AFC) formulation. J Petrol 42, 999–1018.

Steiner, A., Streck, M.J., 2019. Voluminous and compositionally diverse, middle Miocene Strawberry Volcanics of NE Oregon: Magmatism cogenetic with flood basalts of the Columbia River Basalt Group, in: Field Volcanology: A Tribute to the Distinguished Career of Don Swanson. Geological Society of America. https://doi.org/10.1130/2018.2538(03)

Stewart, K., Rogers, N., 1996. Mantle plume and lithosphere contributions to basalts from southern Ethiopia. Earth and Planetary Science Letters 139, 195–211. https://doi.org/10.1016/0012-821X(96)00015-5

Streck, M.J., Grunder, A.L., 2012. Temporal and crustal effects on differentiation of tholeiite to calcalkaline and ferro-trachytic suites, High Lava Plains, Oregon, USA. Geochemistry, Geophysics, Geosystems 13. https://doi.org/10.1029/2012GC004237

Talbot, M.R., Morley, C.K., Tiercelin, J.-J., Le Hérissé, A., Potdevin, J.-L., Le Gall, B., 2004. Hydrocarbon potential of the Meso-Cenozoic Turkana Depression, northern Kenya. II. Source rocks: quality, maturation, depositional environments and structural control. Marine and Petroleum Geology 21, 63–78.

Tefera, M., Chernet, T., Haro, W., Teshome, N., Woldie, K., 1996. Geological map of Ethiopia. Geological Survey of Ethiopia.

Thompson, D.A., Hammond, J.O.S., Kendall, J.-M., Stuart, G.W., Helffrich, G.R., Keir, D., Ayele, A., Goitom, B., 2015. Hydrous upwelling across the mantle transition zone beneath the Afar Triple Junction. Geochemistry, Geophysics, Geosystems 16, 834–846.

Thybo, H., Artemieva, I.M., 2013. Moho and magmatic underplating in continental lithosphere. Tectonophysics 609, 605–619.

Tiercelin, J.-J., Potdevin, J.-L., Thuo, P.K., Abdelfettah, Y., Schuster, M., Bourquin, S., Bellon, H., Clément, J.-P., Guillou, H., Nalpas, T., 2012. Stratigraphy, sedimentology and diagenetic

evolution of the Lapur Sandstone in northern Kenya: Implications for oil exploration of the Meso-Cenozoic Turkana depression. Journal of African Earth Sciences 71, 43–79.

Turner, S.P., Kirstein, L.A., Hawkesworth, C.J., Peate, D.W., Hallinan, S., Mantovani, M.S.M., 1999. Petrogenesis of an 800 m lava sequence in eastern Uruguay: insights into magma chamber processes beneath the Parana flood basalt province. Journal of Geodynamics 28, 471–487.

Ukstins, I.A., Renne, P.R., Wolfenden, E., Baker, J., Ayalew, D., Menzies, M., 2002. Matching conjugate volcanic rifted margins: 40Ar/39Ar chrono-stratigraphy of pre- and syn-rift bimodal flood volcanism in Ethiopia and Yemen. Earth and Planetary Science Letters 198, 289–306. https://doi.org/10.1016/S0012-821X(02)00525-3

Villiger, S., Ulmer, P., Muntener, O., 2004. The Liquid Line of Descent of Anhydrous, Mantle-Derived, Tholeiitic Liquids by Fractional and Equilibrium Crystallization--an Experimental Study at 1{middle dot}0 GPa. Journal of Petrology 45, 2369–2388. https://doi.org/10.1093/petrology/egh042

Wescott, W.A., Wigger, S.T., Stone, D.M., Morley, C.K., 1999. Geology and geophysics of the Lotikipi Plain. Geoscience of Rift Systems-Evolution of East Africa, American Association of Petroleum Geologists Studies in Geology 44, 55–65.

Wilkinson, A.F., 1988. Geology of the Allia Bay area. Report of the Mines and Geology Department, Kenya 54.

WoldeGabriel, G., Yemane, T., Suwa, G., White, T., Asfaw, B., 1991a. Age of volcanism and rifting in the Burji-Soyoma area, Amaro Horst, southern Main Ethiopian Rift: geo- and biochronologic data. Journal of African Earth Sciences (and the Middle East) 13, 437–447. https://doi.org/10.1016/0899-5362(91)90107-A

Wolfenden, E., Ebinger, C., Yirgu, G., Renne, P.R., Kelley, S.P., 2005. Evolution of a volcanic rifted margin: Southern Red Sea, Ethiopia. Geological Society of America Bulletin 117, 846–864.

Yemane, T., Yohunie, T., 1987. Geological Report on sub-sheets A, B, and C (Agere Mariam NG-37-10).

Yu, X., Lee, C.-T.A., Chen, L.-H., Zeng, G., 2015. Magmatic recharge in continental flood basalts: Insights from the Chifeng igneous province in Inner Mongolia: MAGMATIC RECHARGE IN FLOOD BASALT. Geochem. Geophys. Geosyst. 16, 2082–2096. https://doi.org/10.1002/2015GC005805

Zanettin, B., 1978. The evolution of the Chencha escarpment and the Ganjuli graben (lake Abaya) in southern Ethiopian rift. Neues Jahrb. Geol. Paleontol. Monatshefte 8, 473–490.

Zanettin, B., Justin Visentin, E., Bellieni, G., Piccirillo, E.M., Rita, F., 1983. Le volcanisme du Bassin du Nord-Turkana (Kenya): Age, succession et évolution structurale. BCREDP 7, 249–255.

Zanettin, B., Justin-Visentin, E., Nicoletti, M., Piccirillo, E.M., 1980. Correlations among Ethiopian Volcanic Formations with Special References to the Chronological and Stratigraphical problems of the "Trap Series." Accademia Nazionale dei Lincei: Geodynamic Evolution of the Afro-Arabian Rift System: Meeting 47, 231–252.

Figure Captions

Figure 1. Distribution of the Eocene and Oligoene flood basalt provinces in East Africa. Abbreviations: Akobo Basalts (AK), Amaro Region (AM), Chebera (CH), Gidole Horst (GH), Gura Ferda (GF), Kajong (KJ), Lokitaung town (LK), Lotikipi Basin (LT), Nabwal Hills (NB), Yerer Tullu-Wellel Volcanic Lineament (YTVL). Locations for sections 1-7 described in figure 5 correspond to numerals. The distribution of the Akobo Basalts and the Amaro Basalts are not pictured due to their small footprint at the map scale presented here.

Figure 2. Selected bivariant diagrams showing the major and trace element distribution of Eocene flood basalts. Main Series and Makonnen samples broadly conform to the existing geochemical framework of the Amaro Basalt and Gamo Basalt units. The Akobo Basalt is similar to those of the Turkana Eocene lavas (Furman et al., 2006).

Figure 3. Primitive mantle normalised spider diagrams showing the incompatible trace element patterns for flood basalt samples from the Eocene and Oligocene Ethiopian flood basalt provinces with greater than 4% MgO. Fields for existing Amaro, Gamo, and Oligocene HT1 lava compositions were calculated from the 1st and 3rd quartiles. Primitive mantle composition from Sun and McDonough (1989).

Figure 4. Chondrite normalised spider diagrams showing the REE patterns for flood basalt samples from the Eocene and Oligocene Ethiopian flood basalt provinces with greater than 4% MgO. Fields for existing Amaro Basalt, Gamo Basalt, and Oligocene HT1 lava compositions were calculated from the 1st and 3rd quartiles. Chondrite normalization from Boynton (1984). (Pm calculated from geometric mean of Nd-Sm and does not represent analytical values)

Figure 5. Idealized magmatic stratigraphy of southern Ethiopia modified from Rooney (2017). Stratigraphic relationships derived from field observations and geochronology (Davidson and Rex, 1980; Davidson, 1983; Ebinger et al., 1993; George et al., 1998; George and Rogers, 2002; WoldeGabriel et al., 1991). The Akobo Basalt are included in section 4 only to show the temporal relationship between the Gamo-Makonnen unit and the Akobo Basalts.

Figure 6. REAFC controlled-liquid lines of descent (LLD) were calculated for several Amaro lava compositions resulting in a series of solutions that bracket samples of the Gamo-Makonnen magmatic unit. Through REAFC magmatic differentiation, Gamo-Makonnen lava compositions can be derived from a primitive Amaro magma.

Figure 7. Cartoon describing the evolution of the magmatic plumbing system of the Eocene continental LIP. The Akobo Basalts were derived from the destabilization metasomes within the lithospheric mantle in response to the impingement of a mantle plume on the base of the lithosphere. These initial phase lavas are small in volume and restricted in spatial distribution. The Amaro Basalts represent the onset of main phase of volcanism and are the first Eocene continental LIP lavas derived predominantly from sub-lithospheric reservoirs. Increased melt contributions from the plume feed a magmatic plumbing system that is poorly connected and inefficient at processing magmas. The resultant lavas are mostly primitive but heterogenous in composition. Poor conductivity of recharging magma results in localized advanced differentiation evidenced by the Arba Minch Tuff. The early stages of the Gamo-Makonnen were the onset of an efficient magma plumbing system likely fed by an increased supply of magma. Abundant, interconnected magma chambers efficiently differentiate and homogenize magmas during this period. The resulting lavas were homogenous and modestly lava

compositions observed in the Gamo-Makonnen magmatic unit. During the Gamo-Makonnen late stage, the magmatic plumbing system was more efficient at differentiating magmas, resulting in the progressively more evolved lavas observed in the Gamo Basalts (George and Rogers, 2002). Eventual shut-down of the magmatic system is heralded by the eruption of the widespread Amaro Tuff, the result of advanced differentiation possible due to a lack of magma recharge.
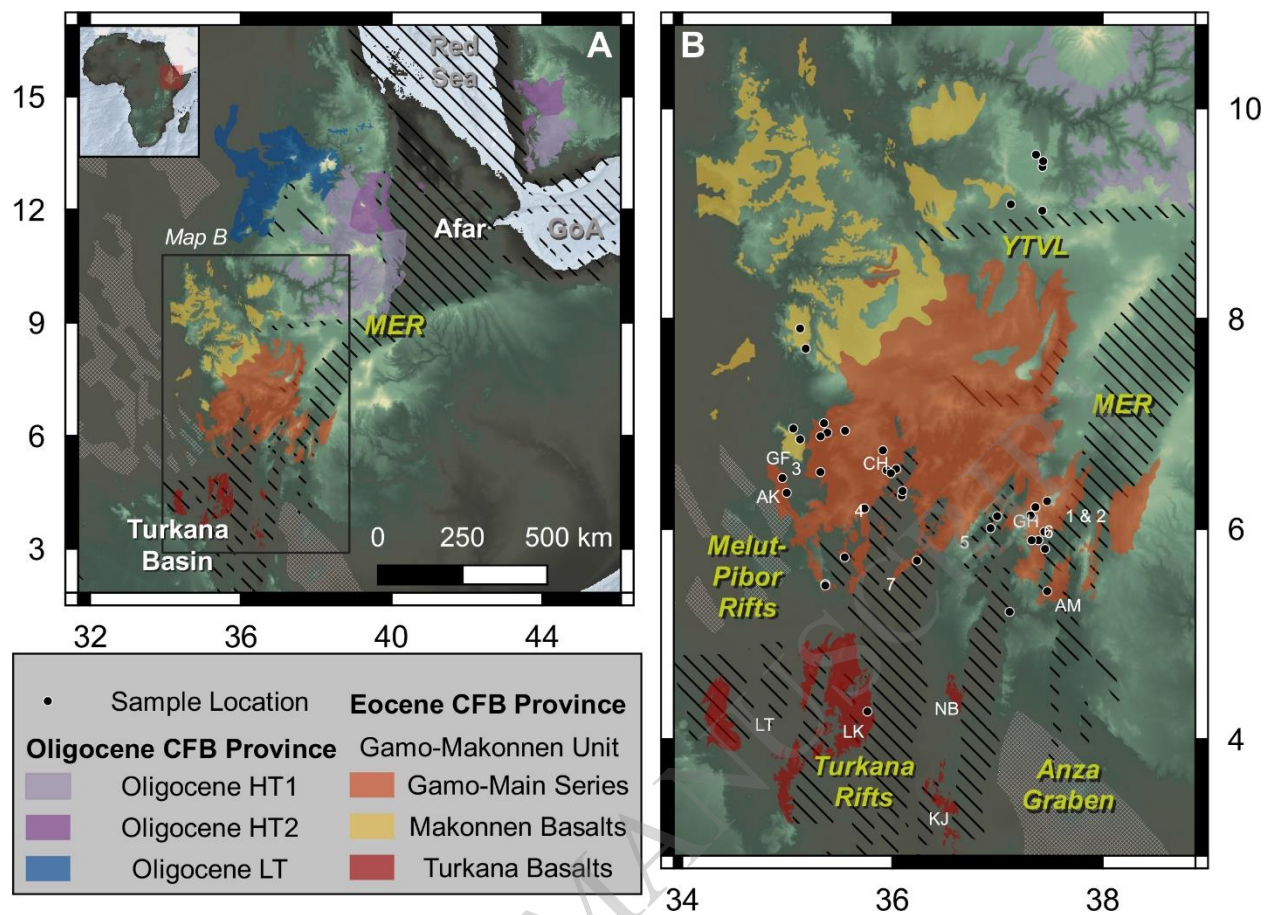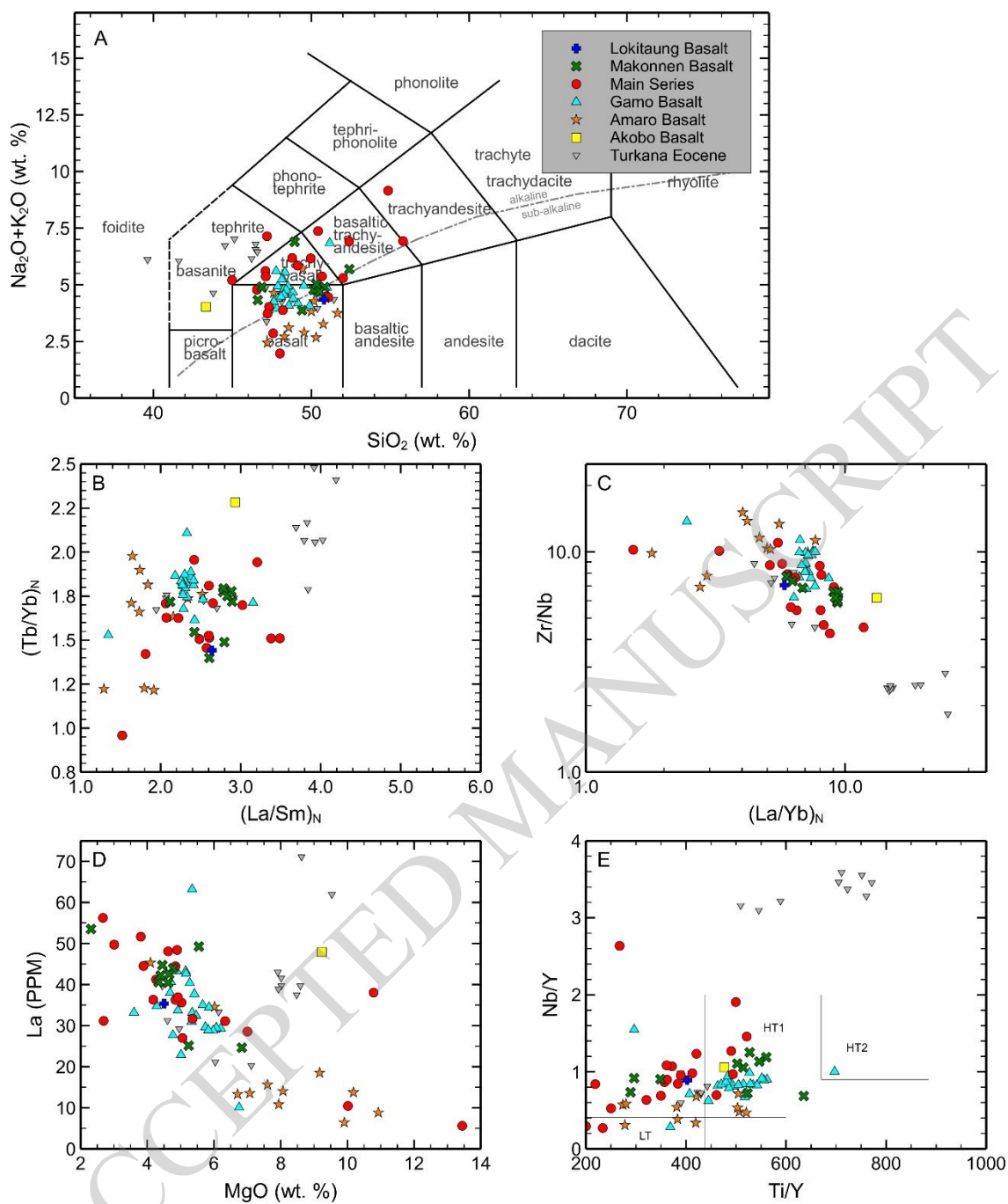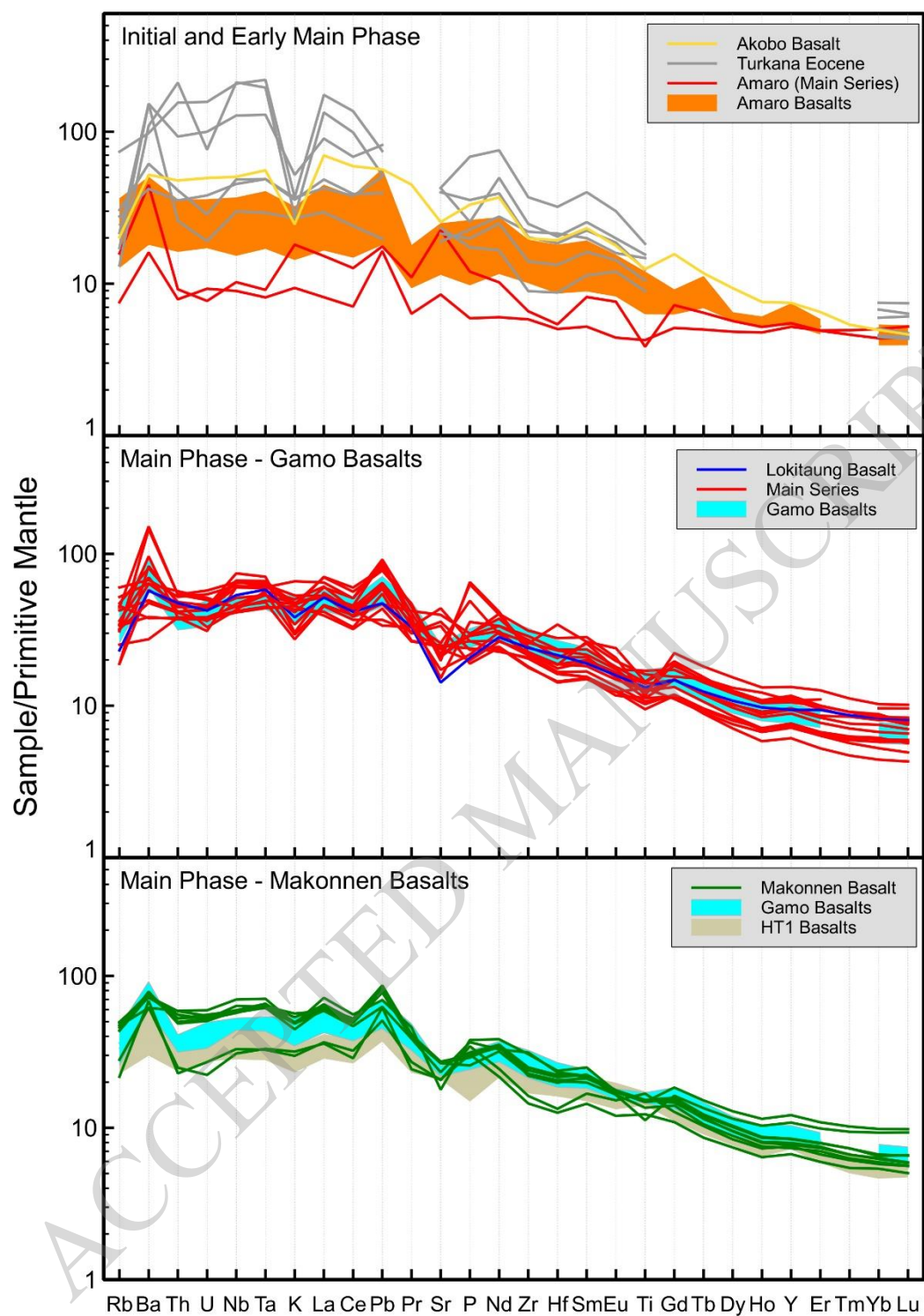
Figure 1

Figure 2

Figure 3
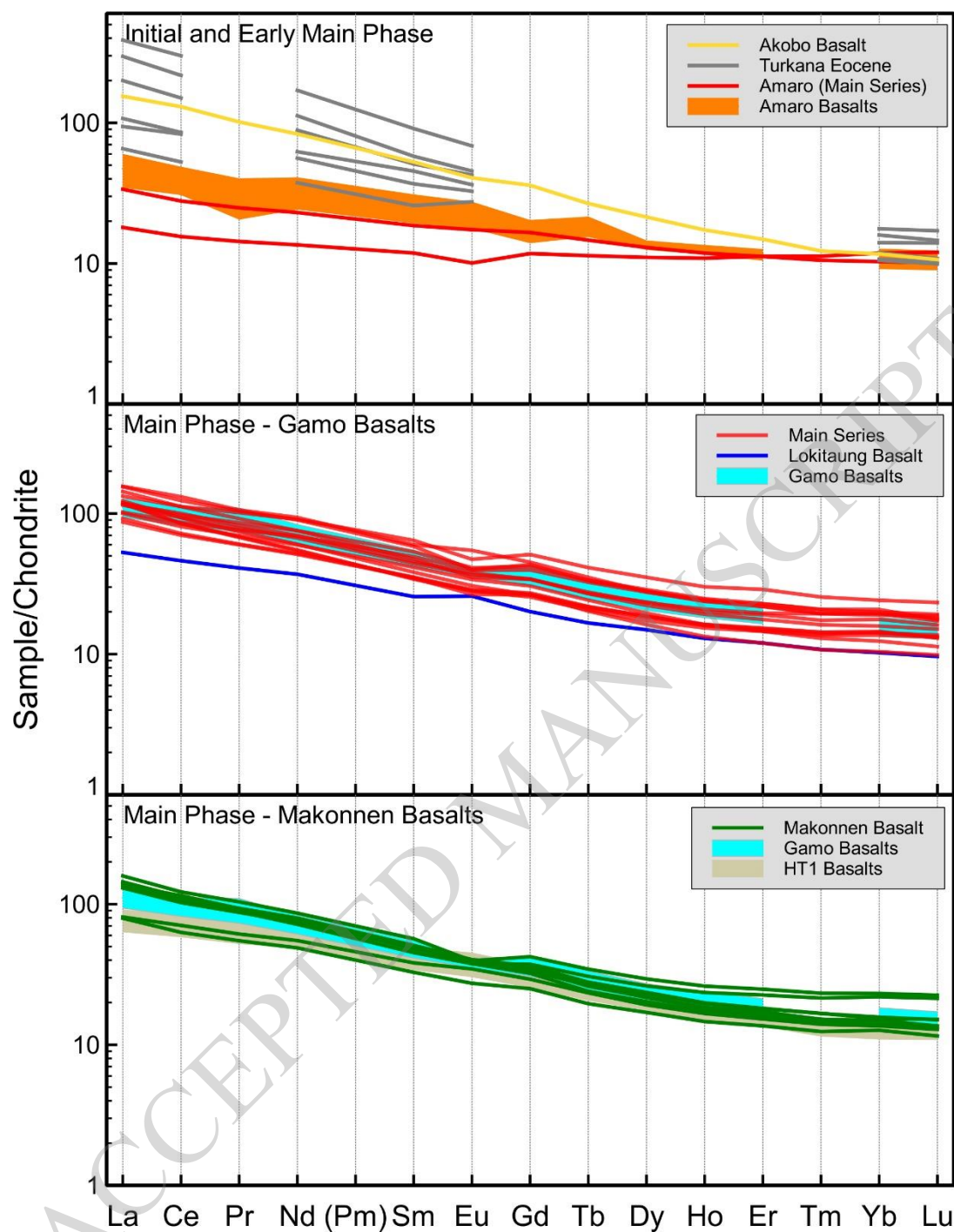
Figure 4

Figure 5

Figure 6

Figure 7